

Synthesis, characterization, biological activity, and 3D-QSAR studies on some novel class of pyrrole derivatives as antitubercular agents

Shrinivas D. Joshi · Uttam A. More ·
Sheshagiri R. Dixit · Haresh H. Korat ·
Tejraj M. Aminabhavi · Aravind M. Badiger

Received: 12 December 2012 / Accepted: 10 August 2013 / Published online: 25 August 2013
© Springer Science+Business Media New York 2013

Abstract A new series of pyrrole derivatives have been designed, synthesized, and their structures have been elucidated along with the evaluation of antitubercular activity against *Mycobacterium tuberculosis* H₃₇Rv using the microplate alamar blue assay method and antibacterial activity against *Staphylococcus aureus*, *Bacillus subtilis*, *Klebsiella pneumoniae*, and *Escherichia coli* by broth micro-dilution assay method. Structural activity relationships and 3D-QSAR analysis have been carried out by Topomer Comparative Molecular Field Analysis (CoMFA). Training set of 42 and test set of 8 active compounds were used to develop the method that showed cross-validated correlation coefficient (q^2) of 0.815, standard error of prediction of 0.36, non-cross-validated correlation coefficient (r^2) of 0.973, and standard error of estimate of 0.14 with six components.

Keywords Pyrroles · Antibacterial activity · Antitubercular activity · Broth dilution assay method · Cytotoxicity · Topomer CoMFA

Introduction

Tuberculosis (TB), a lung infection caused mainly by *Mycobacterium tuberculosis* (MTB), is a leading infectious disease claiming millions of death, mostly in developing countries (Duncan and Barry, 2004; World Health Organization [WHO], 2008). According to the WHO reports one-third of the world's population is currently infected with TB bacillus, each year 8 million people worldwide develop active TB and about 1.7 million people die (Valadas and Antunes, 2005). TB drugs available today in the market have been discovered mainly during 1945–1965, but since then innumerable new drugs have been developed as well as drug-resistant strains of mycobacterium have emerged in medical area. Multidrug-resistant TB and extensive drug-resistant TB are the most dangerous forms of TB that are resistant to isoniazid and rifampicin. This has created greater challenges for the treatment of TB, creating a need to develop new therapeutic agents. Among the many organic moieties, pyrrole is the widely explored heterocycle in plant and animal kingdom.

Pyrrole and its derivatives possess antitumor (Kamal *et al.*, 2012), analgesic (Ahmadi *et al.*, 2011), antitubercular (Biava *et al.*, 2010; Sbardella *et al.*, 2004), and anti-inflammatory activities (Mohamed *et al.*, 2011). Several macromolecular antibiotics having pyrrole structure have been isolated from the biological sources and their activities have been identified (Jones and Bean, 1997; Jones, 1992). Recently, pyrrole derivatives have emerged as chemotherapeutic agents potentially useful for inhibiting the activities of MTB and other atypical mycobacteria, including *M. avium* complex, an opportunistic pathogen that greatly contributes to the death of AIDS patients.

Lipophilicity is a key property that influences the ability of a drug to reach the target by transmembrane diffusion and to

S. D. Joshi (✉) · U. A. More · S. R. Dixit ·
H. H. Korat · T. M. Aminabhavi
Novel Drug Design and Discovery Laboratory, Department of
Pharmaceutical Chemistry, S.E.T.'s College of Pharmacy,
Sangolli Rayanna Nagar, Hubli-Dharwar 580 002, India
e-mail: shrinivasdj@rediffmail.com; shrinivasdj23@gmail.com

U. A. More
Centre for Research and Development, Prist University,
Thanjavur 613 403, Tamil Nadu, India

A. M. Badiger
BDR Pharmaceuticals International Pvt. Ltd.,
Baroda 390 021, India

have a major effect on the biological activity. The azole antituberculars are regarded as the emerging class of thiazoles known as lipophilic analogs similar to imidazoles. Thiazoles are utilized as pharmacophores due to their favorable metabolic profile and their ability to engage in hydrogen-bonding. Biological activities of thiazole ring systems have been well documented (Gorzynski *et al.*, 2004; Vicini *et al.*, 2003). On the other hand, pyrrolylimido group has been widely used in drug discovery due to its wide range of pharmacological and biological activities such as anti-inflammatory, analgesic, antispasmodic, antibacterial, antifungal, etc. (Abdel-Aziz, 2007; Borchhardt and Andricopulo, 2009).

In drug design and discovery area, CoMFA (Comparative Molecular Field Analysis), a 3D-QSAR technique, has been the widely used computational tool (Cramer *et al.*, 1988), since it is capable of predicting the biological activity of new chemical entities by establishing the relationship between steric/electrostatic properties and the biological activities in the form of contour maps. The present work is a continuation of our ongoing research on the biologically active molecules such as pyrrole derivatives (Joshi *et al.*, 2008, 2010, 2013a,b). Herein, we report the synthesis and characterization of some novel type of pyrrolylimido as well as thiazole derivatives and estimate their antibacterial and antitubercular activities.

3D-QSAR study

Computational details

The 3D-QSAR techniques of Topomer CoMFA have been carried out with Tripos SYBYL-X 2.0 (Sybyl-X 2.0, 2012) running on a Intel® Core™ i3-2130 CPU@ 3.40 GHz processor using Windows 7 professional software. The activity dataset consisted of 50 molecules (Tables 1 and 2). The measurement of antitubercular activity used to develop the Topomer CoMFA have been expressed as $\text{pMIC} = -\log(\text{MIC})$, where MIC is minimum inhibitory concentration values that were changed to minus logarithmic scale value pMIC, as a dependent variable for Topomer CoMFA analysis. Then the antitubercular activity data were converted into logarithmic scale as the resulting model behaves more reasonably that will offer better linear models.

The dataset was divided into a training set of 42 molecules and test set of 8 molecules on the basis of biological diversity, such that both the training and test sets consist of high-, medium-, and low-activity molecules. All the dataset molecules were sketched by the SKETCH module implemented in the SYBYL program and ligand geometries were optimized by energy minimization with Powel method using the Tripos forcefield. They were then subjected to simulated annealing to get a stable conformation.

Simulated annealing was performed for each ligand up to 200 cycles with default parameters and then conformations were sorted out according to the least potential energy value, which were minimized with quantum mechanical semi-empirical AM1 (Austin Model 1) method using MOPAC (Molecular Orbital PACKage). Atomic charges were calculated using the MMFF94 (Merck Molecular Force Field) method for Topomer structure and dataset was then used for Topomer CoMFA analysis.

Topomer CoMFA

Topomer CoMFA is a technique introduced by Cramer, which has two main phases, the first being generation of the topomer 3D models for each of the “side chains” and the second one is the CoMFA analysis itself (Cramer, 2003). It delineates the need for alignment, which is mandatory for typical CoMFA analysis. Topomer CoMFA has both graphical and statistical results. Concerning the graphical results, it was used to construct stdev/coeff contour maps to show field effects on the target features. The contour plots are beneficial to identify important regions where some changes in steric or electrostatic fields can affect the biological activity. The maps generated depict regions having scaled coefficients $>80\%$ (favored) or $<20\%$ (disfavored).

In Topomer CoMFA analysis, all molecules of the dataset were separated into two fragments shown as R_1 (red) and R_2 (blue) groups in Fig. 1. Two template molecules were chosen for fragmentation, one from pyrrolylimide **5h** and another from pyrrolylthiazole **13h** (Fig. 2), which are the most active compounds of their respective series and are having low-energy conformation. Each Topomer fragment was applied with topomer alignment to make a 3D invariant representation (Cramer *et al.*, 1996). Steric and electrostatic interaction energies were calculated using a carbon sp^3 probe.

Partial least square (PLS) analysis

The PLS method was used to set up a correlation between the molecular fields and inhibitory activity of the molecules (Cramer, 1993). Topomer CoMFA descriptors were used as independent variable and the log activities as the dependent variable in a PLS regression analysis. The optimum number of components was determined with SAMPLS (samples-distance PLS) (Bush and Nachbar Jr, 1993). The cross-validation was carried out by the leave-one-out (LOO) method, in which one molecule is removed from the dataset and its activity is predicted using the model derived from rest of the molecules in the dataset. The q^2 resulted in an optimum number of components and the lowest standard error of prediction (StdErr). The equations for q^2 and standard errors are given below.

Table 1 Antitubercular activity of a novel series of pyrrolylimides (**5a–m**) and (**8a–m**)

Compound		pMIC	Compound		pMIC
5a		5.20	8a		4.90
5b		5.20	8b*		5.10
5c		6.10	8c		5.51
5d		5.51	8d		5.51
5e		6.40	8e		6.40
5f		6.10	8f		6.40
5g*		6.40	8g		6.40
5h		6.70	8h		6.70
5i		6.10	8i		6.10
5j		5.51	8j		5.20
5k*		5.33	8k		5.20
5l		5.51	8l*		5.36
5m		5.51	8m		5.20

Asterisk (*) indicates test set compounds.

$$q^2 = 1 - \frac{\sum_y (Y_{\text{pred}} - Y_{\text{actual}})^2}{\sum_y (Y_{\text{actual}} - Y_{\text{mean}})^2},$$

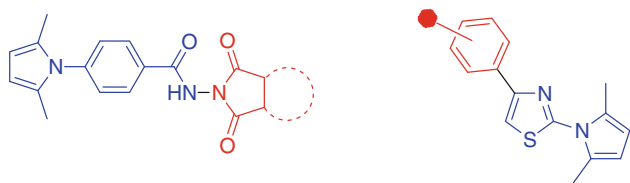
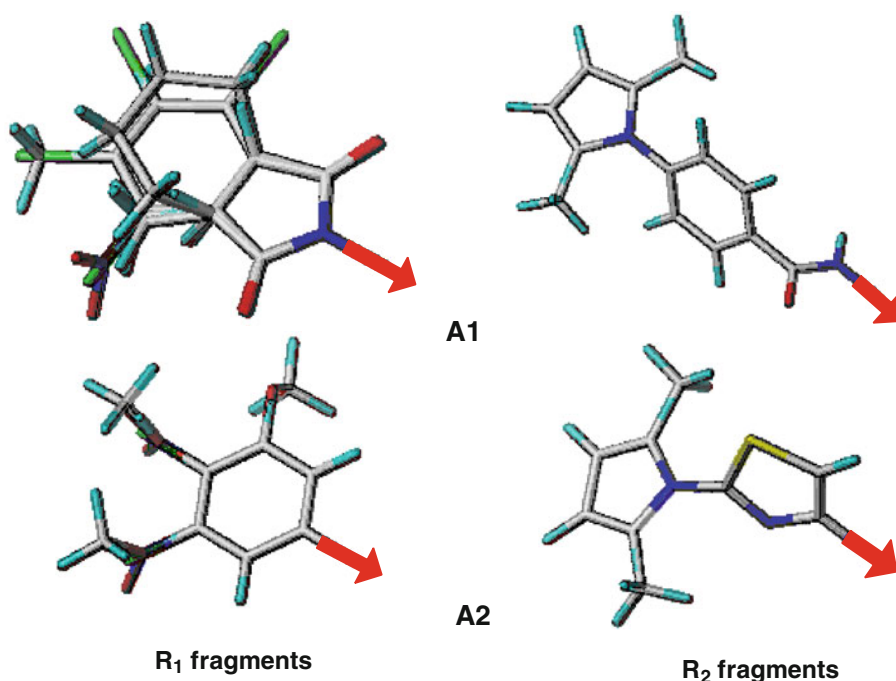
where Y_{pred} is predicted activity, Y_{actual} is experimental activity, and Y_{mean} is the best estimate of the mean.

$$\text{SEE, SEP} = \sqrt{\frac{\text{PRESS}}{n - c - 1}},$$

where n is number of compounds, c is number of components, and $\text{PRESS} = \sum_y (Y_{\text{pred}} - Y_{\text{actual}})^2$.

Table 2 Antitubercular activity of a novel series of pyrrolylthiazoles (**12a–l**) and (**13a–l**)

Compound	R	pMIC	Compound	R	pMIC
12a	-4H	6.40	13a	-4H	6.40
12b	-4Cl	6.40	13b	-4Cl	6.10
12c	-4OH	4.30	13c	-4OH	4.90
12d	-4Br	6.10	13d	-4Br	6.40
12e	-4OCH ₃	4.90	13e	-4OCH ₃	5.20
12f	-4NO ₂	6.40	13f	-4NO ₂	6.40
12g^a	-4NH ₂	4.60	13g	-4NH ₂	4.90
12h	-4F	6.70	13h	-4F	6.70
12i	-2,4-dichloro	6.40	13i	-2,4-dichloro	6.40
12j	-3,4,5-(OCH ₃) ₃	4.30	13j^a	-3,4,5-(OCH ₃) ₃	4.90
12k^a	-3,4-(OCH ₃) ₂	4.30	13k	-3,4-(OCH ₃) ₂	4.30
12l	-3-NO ₂	6.10	13l^a	-3-NO ₂	6.40

^a Test set compounds**Fig. 1** R₁ fragment is represented by the red color and R₂ fragment is represented by blue color (Color figure online)**Fig. 2** Topological alignment of R₁ and R₂ fragments generated by Topomer CoMFA analysisPredictive correlation coefficient (r_{pred}^2)

The predictive ability of 3D-QSAR model was determined from test set of eight molecules not included in the model generation. The predictive correlation coefficient (r_{pred}^2), based on the test set molecules is defined as:

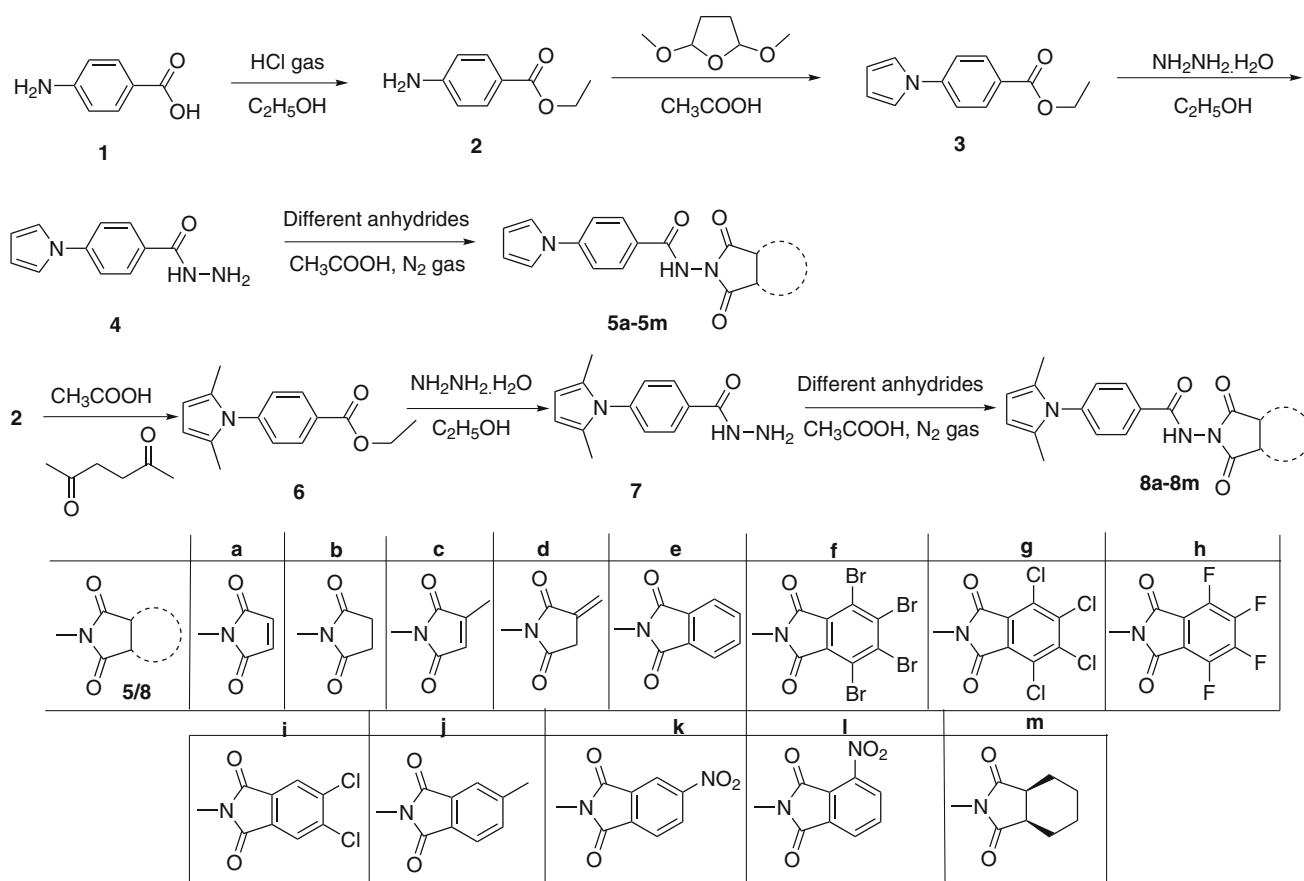
$$r_{\text{pred}}^2 = \frac{(SD - \text{PRESS})}{SD},$$

where SD is the sum of squared deviations between the biological activity of the test set and the mean activity of the training set molecules, PRESS is the sum of squared deviations between the predicted and the actual activity values for every molecule in the test set.

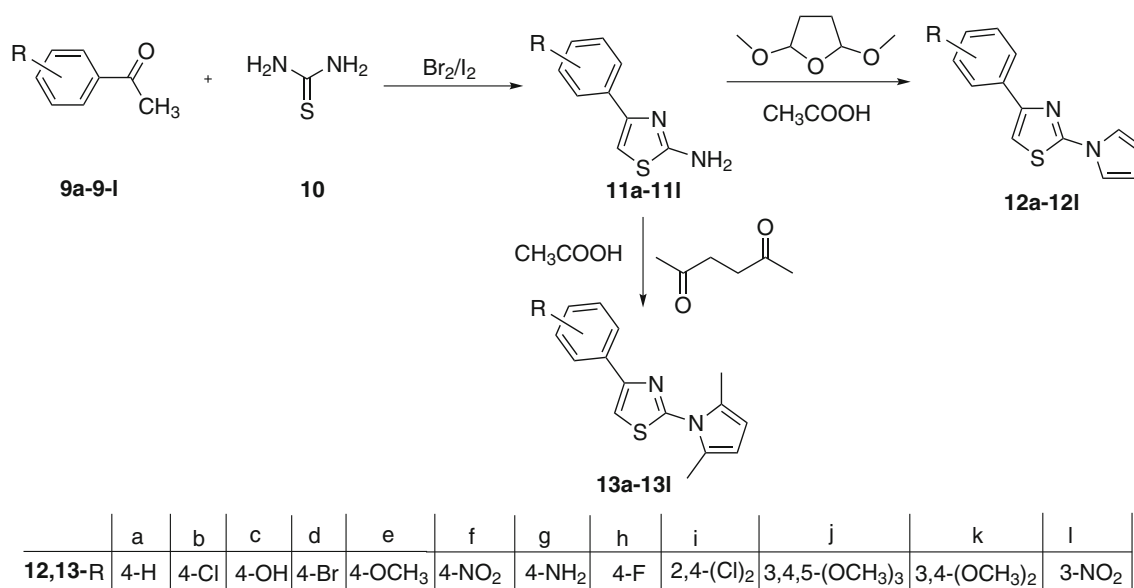
Materials and methods

Chemistry

Compounds **5a–m**, **8a–m**, **12a–l**, and **13a–l** were prepared as per Schemes 1 and 2. The compounds *N*-(substituted)-4-(1*H*-pyrrol-1-yl)benzamides (**5a–m**) were synthesized from the commercially available 4-aminobenzoic acid (**1**) (Scheme 1). 4-Aminobenzoic acid (**1**) was subjected to esterification reaction in ethanol and HCl gas to give ethyl 4-aminobenzoate (**2**). Ethyl 4-aminobenzoate (**2**) was subjected to *Paal–Knorr* reaction with 2,5-dimethoxytetrahydrofuran in dried acetic acid to give ethyl 4-(1*H*-pyrrol-1-yl)benzoate (**3**). Hydrazinolysis of ethyl 4-(1*H*-



Scheme 1 Synthetic route of a novel series of pyrrolylimides

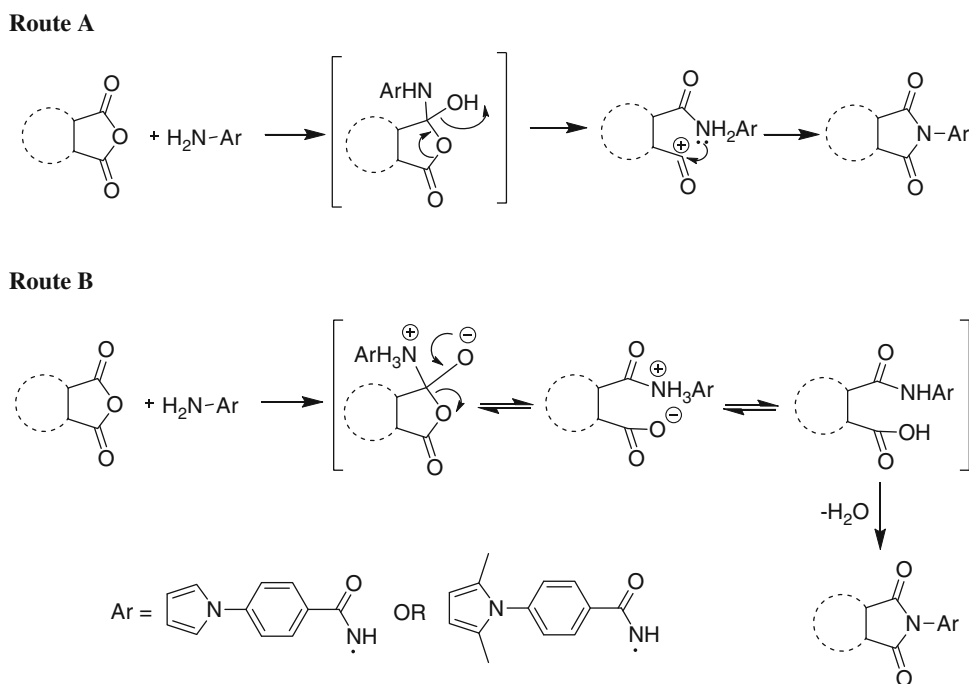


Scheme 2 Synthetic route of a novel series of pyrrolylthiazoles

pyrrol-1-yl)benzoate (**3**) with hydrazine hydrate in ethanol gave 4-(1*H*-pyrrol-1-yl)benzoic acid hydrazide (**4**). The *N*-(substituted)-4-(1*H*-pyrrol-1-yl)benzamide compounds

(**5a–m**; Scheme 1) were prepared by cyclodehydration of 4-(1*H*-pyrrol-1-yl)benzoic acid hydrazide (**4**) with different anhydrides in dried acetic acid media under nitrogen

Scheme 3 Routes for the mechanism of formation of pyrrolylimide derivatives **5a–m** and **8a–m**



atmosphere. *Paal–Knorr* condensation reaction between ethyl 4-aminobenzoate (**2**) and 2,5-hexanedione in glacial acetic acid furnished the ethyl 4-(2,5-dimethyl-1*H*-pyrrol-1-yl)benzoate (**6**). Nucleophilic reaction of hydrazine hydrate with the ester **6** in ethanolic medium produced 4-(2,5-dimethyl-1*H*-pyrrol-1-yl)benzoic acid hydrazide (**7**). The *N*-(substituted)-4-(2,5-dimethyl-1*H*-pyrrol-1-yl)benzamides (**8a–m**) were synthesized by cyclodehydration of **7** with different anhydrides in dried acetic acid under nitrogen atmosphere.

In Scheme 2, 2-amino-4-(4-substituted phenyl)thiazoles (**11a–l**) were synthesized as described previously in which 4-substituted acetophenones (**9a–l**) were used as the starting materials. Compounds (**9a–l**) were condensed with thiourea (**10**) in the presence of iodine or bromine as a catalyst, to give the key compounds; viz 2-amino-4-(4-substituted phenyl)thiazoles (**11a–l**). 4-(4-Substituted phenyl)-2-(1*H*-pyrrol-1-yl)thiazoles (**12a–l**; Scheme 2) and 4-(4-substituted phenyl)-2-(2,5-dimethyl-1*H*-pyrrol-1-yl)thiazoles (**13a–l**; Scheme 2) were synthesized by *Paal–Knorr* reaction of thiazoles (**11a–l**) with 2,5-dimethoxytetrahydrofuran and 2,5-hexanedione, respectively, in dried glacial acetic acid.

The cyclic imide formation possibly takes place according to one of the two mechanism routes shown in Scheme 3. The possible mechanism for *Paal–Knorr* pyrrole synthesis is depicted in Scheme 4.

Experimental

Chemicals used in the synthesis of the compounds were purchased from Sigma-Aldrich, S. D. Fine-Chem

Limited, and Spectrochem Pvt. Ltd. Solvents were of reagent grade and when necessary these were purified and dried by the standard methods. Melting points (mp) of the synthesized compounds were determined by Shital Scientific Industries mp apparatus and are uncorrected. Infrared spectra were recorded on a Bruker spectrophotometer using the KBr pellets. The ¹H and ¹³C NMR spectra were recorded on Bruker AVANCE II 400 MHz and Bruker AVANCE III 500 MHz instruments using dimethylsulfoxide (DMSO-*d*₆) solvent and TMS as an internal standard. The chemical shifts are expressed as δ values (ppm).

Mass spectra (MS) were taken in JEOL GCMATE II GC-Mass spectrometer and Waters Micromass Q-ToF Micro LC-Mass spectrometer. All the compounds exhibited spectral data consistent with the proposed structures and values of microanalysis were within ± 0.4 % of the theoretical values. Analytical thin-layer chromatography (TLC) was performed on the precoated TLC sheets of silica gel 60 F₂₅₄ (Merck, Darmstadt, Germany) visualized by long- and short-wavelength ultraviolet lamps. Chromatographic purifications were performed on Merck aluminum oxide (70–230 mesh) and Merck silica gel (70–230 mesh).

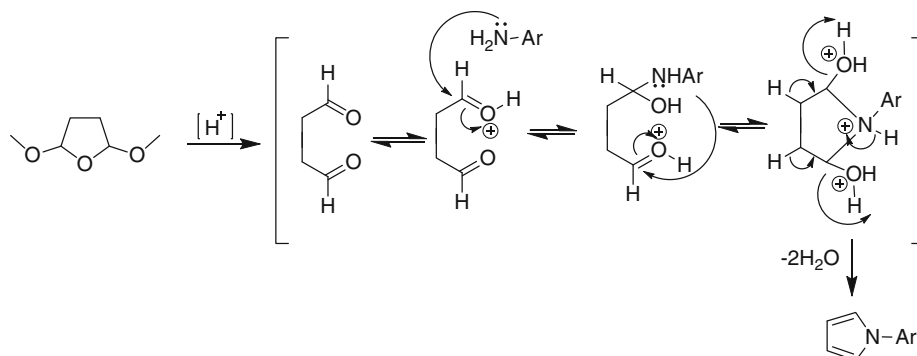
Synthesis of 4-(1*H*-pyrrol-1-yl)benzoic acid hydrazide (**4**)

Ethyl 4-(1*H*-pyrrol-1-yl)benzoate (**3**; 15 mmol) was refluxed with hydrazine hydrate (10 mL) in absolute ethanol (10 mL) for 3 h. The reaction mixture was cooled and

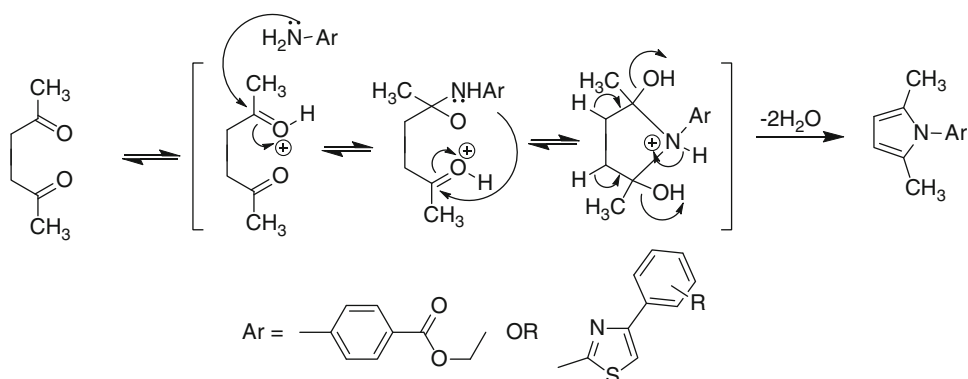
Scheme 4 Routes for the mechanism of formation of pyrrole derivatives **3**, **6**, **12a–l**, and **13a–l**

Paal-Knorr Pyrrole Synthesis Mechanism

Route A



Route B



the crystalline mass obtained was further recrystallized from ethanol.

Yield 74 %. mp 180–182 °C (Joshi *et al.*, 2008).

General procedure for the preparation of N-(substituted)-4-(1H-pyrrol-1-yl)benzamides (5a–m)

Mixture of 4-(1H-pyrrol-1-yl)benzohydrazide (25 mmol) and anhydride (25 mmol) in 10 mL dried acetic acid was stirred for 30 min at room temperature. The separated solid was filtered, washed with diethyl ether, and dried. The solid was dissolved in 30 mL dried acetic acid and stirred overnight under nitrogen atmosphere. The reaction mixture was then poured into ice-cold water; the separated solid was collected, washed with water, dried, and recrystallized by aqueous DMF to get the desired product **5a–m**.

N-(2,5-dioxo-2,5-dihydro-1H-pyrrol-1-yl)-4-(1H-pyrrol-1-yl)benzamide (5a) Yield 43 %. mp 198–200 °C; FTIR (KBr): 3215 (NH), 3105, 2999 (Ar–H), 1717 (2,5-dihydropyrrole C=O), 1655 (2,5-dihydropyrrole C=O), 1630 (amide C=O) cm^{-1} ; ^1H NMR (500 MHz, $\text{DMSO-}d_6$) δ

ppm: 6.32 (dd, 2H, pyrrole–C₃ and C₄–H), 7.51 (dd, 2H, pyrrole–C₂ and C₅–H), 7.75 (d, 2H, $J = 5$ Hz, Ph–C₃ and C₅–H), 8.00 (d, 2H, $J = 10$ Hz, Ph–C₂ and C₆–H), 10.64 (s, 2H, 2,5-dihydropyrrole–C₃ and C₄–H), 13.05 (s, 1H, amide–NH); ^{13}C NMR (500 MHz, $\text{DMSO-}d_6$) δ ppm: 167.41 (amide–C=O), 164.92 (2,5-dihydropyrrole–C₂), 163.76 (2,5-dihydropyrrole–C₅), 142.82 (Ph–C₄), 133.57 (2,5-dihydropyrrole–C₃ and C₄), 129.68 (Ph–C₃ and C₅), 128.87 (Ph–C₁), 119.47 (Ph–C₂ and C₆), 118.92 (pyrrole–C₂ and C₃), 111.70 (pyrrole–C₃ and C₄); MS (ESI): m/z = found 281.08 [M^+], 216, 171; calcd. 281.27. Anal. $\text{C}_{15}\text{H}_{11}\text{N}_3\text{O}_3$.

N-(2,5-dioxopyrrolidin-1-yl)-4-(1H-pyrrol-1-yl)benzamide (5b) Yield 41 %. mp 228–230 °C; FTIR (KBr): 3221 (NH), 3036, 2967 (Ar–H), 1694 (pyrrolidine C=O), 1646 (amide C=O) cm^{-1} ; ^1H NMR (500 MHz, $\text{DMSO-}d_6$) δ ppm: 2.46–2.51 (m, 4H, pyrrolidine–C₃ and C₄–H), 6.32 (dd, 2H, pyrrole–C₃ and C₄–H), 7.50 (dd, 2H, pyrrole–C₂ and C₅–H), 7.73 (d, 2H, $J = 5$ Hz, Ph–C₃ and C₅–H), 7.98 (d, 2H, $J = 10$ Hz, Ph–C₂ and C₆–H), 9.93 (s, 1H, amide–NH); ^{13}C NMR (500 MHz, $\text{DMSO-}d_6$) δ ppm: 174.02

(pyrrolidine-C₂), 171.04 (pyrrolidine-C₅), 165.08 (amide-C=O), 142.69 (Ph-C₄), 129.57 (Ph-C₃ and C₅), 129.19 (Ph-C₁), 119.45 (Ph-C₂ and C₆), 118.90 (pyrrole-C₂ and C₅), 111.65 (pyrrole-C₃ and C₄), 29.29 (pyrrolidine-C₃), 28.64 (pyrrolidine-C₄); MS (ESI): *m/z* = found 283.10 [M⁺], 186; calcd. 283.28. Anal. C₁₅H₁₃N₃O₃.

N-(3-methyl-2,5-dioxo-2,5-dihydro-1*H*-pyrrol-1-yl)-4-(1*H*-pyrrol-1-yl)benzamide (**5c**) Yield 65 %. mp 178–180 °C; FTIR (KBr): 3370 (NH), 3099, 2924 (Ar-H), 1733 (2,5-dihydropyrrole C=O), 1608 (amide C=O) cm⁻¹; ¹H NMR (400 MHz, CDCl₃) δ ppm: 2.13 (s, 3H, CH₃ at 2,5-dihydropyrrole-C₃), 6.32 (dd, 2H, pyrrole-C₃ and C₄-H), 6.64 (s, 1H, 2,5-dihydropyrrole-C₃-H), 7.30 (dd, 2H, pyrrole-C₂ and C₅-H), 7.61 (d, 2H, *J* = 8 Hz, Ph-C₃ and C₅-H), 8.07 (d, 2H, *J* = 8 Hz, Ph-C₂ and C₆-H), 10.94 (s, 1H, amide-NH); ¹³C NMR (400 MHz, CDCl₃) δ ppm: 168.77 (amide-C=O), 167.54 (2,5-dihydropyrrole-C₂), 164.54 (2,5-dihydropyrrole-C₅), 144.53 (2,5-dihydropyrrole-C₃), 142.84 (Ph-C₄), 129.43 (Ph-C₂ and C₆, 2,5-dihydropyrrole-C₄), 126.97 (Ph-C₃ and C₅), 126.52 (Ph-C₁), 118.49 (pyrrole-C₃ and C₄), 111.11 (pyrrole-C₂ and C₅), 10.99 (CH₃ of 2,5-dihydropyrrole-C₃); MS (ESI): *m/z* = found 296.10 [M⁺+1], 299, 281, 267, 216, 170; calcd. 295.29. Anal. C₁₆H₁₃N₃O₃.

N-(3-methylene-2,5-dioxopyrrolidin-1-yl)-4-(1*H*-pyrrol-1-yl)benzamide (**5d**) Yield 80 %. mp 202–204 °C; FTIR (KBr): 3202 (NH), 3026, 2917 (Ar-H), 1680 (pyrrolidine C=O), 1630 (amide C=O) cm⁻¹; ¹H NMR (400 MHz, DMSO-*d*₆) δ ppm: 5.78 (d, 2H, CH₂ at pyrrolidine-C₃), 6.21 (d, 2H, CH₂ at pyrrolidine-C₄), 6.26 (dd, 2H, pyrrole-C₃ and C₄-H), 7.23 (dd, 2H, pyrrole-C₂ and C₅-H), 7.54 (d, 2H, *J* = 12 Hz, Ph-C₃ and C₅-H), 7.98 (d, 2H, *J* = 8 Hz, Ph-C₂ and C₆-H), 9.91 (s, 1H, amide-NH); ¹³C NMR (400 MHz, DMSO-*d*₆) δ ppm: 168.87 (amide-C=O), 167.46 (pyrrolidine-C₂), 164.63 (pyrrolidine-C₅), 142.26 (Ph-C₄), 135.02 (pyrrolidine-C₃), 129.12 (CH₂ at pyrrolidine-C₃), 128.76 (Ph-C₃ and C₅), 127.12 (Ph-C₁), 118.52 (Ph-C₂ and C₆), 118.44 (pyrrole-C₂ and C₅), 110.95 (pyrrole-C₃ and C₄), 36.53 (pyrrolidine-C₄); MS (ESI): *m/z* = found 295.10 [M⁺], 297, 171, 154; calcd. 295.29. Anal. C₁₆H₁₃N₃O₃.

N-(1,3-dioxoisindolin-2-yl)-4-(1*H*-pyrrol-1-yl)benzamide (**5e**) Yield 75 %. mp 189–190 °C; FTIR (KBr): 3368 (NH), 3141, 2985 (Ar-H), 1728 (isoindoline C=O), 1672 (amide C=O) cm⁻¹; ¹H NMR (400 MHz, DMSO-*d*₆) δ ppm: 6.35 (dd, 2H, pyrrole-C₃ and C₄-H), 7.32 (dd, 2H, pyrrole-C₂ and C₅-H), 7.64 (d, 2H, *J* = 8 Hz, Ph-C₃ and C₅-H), 7.89–7.97 (m, 4H, isoindoline-C₄, C₅, C₆ and C₇-H), 8.13 (d, 2H, *J* = 8 Hz, Ph-C₂ and C₆-H), 11.20 (s, 1H, amide-NH); ¹³C NMR (500 MHz, CDCl₃) δ ppm: 167.18 (amide-C=O), 165.38 (isoindoline-C₃), 164.52

(isoindoline-C₁), 134.83 (isoindoline-C₅, C₆, C₈ and C₉), 130.13 (Ph-C₄), 129.54 (Ph-C₃ and C₅), 124.15 (Ph-C₁, C₂ and C₆), 119.65 (isoindoline-C₄ and C₇), 119.01 (pyrrole-C₂ and C₅), 111.70 (pyrrole-C₃ and C₄); MS (ESI): *m/z* = found 331.10 [M⁺], 266, 186, 119, 102, 78; calcd. 331.32. Anal. C₁₉H₁₃N₃O₃.

N-(4,5,6,7-tetrabromo-1,3-dioxoisindolin-2-yl)-4-(1*H*-pyrrol-1-yl)benzamide (**5f**) Yield 47 %. mp 282–284 °C; FTIR (KBr): 3258 (NH), 3041, 2981 (Ar-H), 1784 (isoindoline C=O), 1741 (isoindoline C=O), 1699 (amide C=O) cm⁻¹; ¹H NMR (400 MHz, DMSO-*d*₆) δ ppm: 6.15 (dd, 2H, pyrrole-C₃ and C₄-H), 7.24 (dd, 2H, pyrrole-C₂ and C₅-H), 7.55 (d, 2H, *J* = 8 Hz, Ph-C₃ and C₅-H), 7.93 (d, 2H, *J* = 12 Hz, Ph-C₂ and C₆-H), 11.24 (s, 1H, amide-NH); ¹³C NMR (400 MHz, DMSO-*d*₆) δ ppm: 171.90 (amide-C=O), 164.39 (isoindoline-C₃), 161.14 (isoindoline-C₁), 143.04 (Ph-C₄), 137.65 (isoindoline-C₈ and C₉), 129.65 (isoindoline-C₅ and C₆), 128.81 (Ph-C₃ and C₅), 126.67 (isoindoline-C₄ and C₇), 121.40 (Ph-C₁), 118.73 (Ph-C₂ and C₆), 118.59 (pyrrole-C₂ and C₅), 111.26 (pyrrole-C₃ and C₄); MS (ESI): *m/z* = found 646.73 [M⁺], 644.74 [M⁺-2], 648.73 [M⁺+2], 580/578, 568/566, 488/486, 406, 326, 248, 150, 120, 105, 84; calcd. 646.91. Anal. C₁₉H₉Br₄N₃O₃.

4-(1*H*-pyrrol-1-yl)-*N*-(4,5,6,7-tetrachloro-1,3-dioxoisindolin-2-yl)benzamide (**5g**) Yield 49 %. mp 298–300 °C; FTIR (KBr): 3233 (NH), 3017, 2981 (Ar-H), 1787 (isoindoline C=O), 1750 (isoindoline C=O), 1699 (amide C=O) cm⁻¹; ¹H NMR (400 MHz, DMSO-*d*₆) δ ppm: 6.40 (dd, 2H, pyrrole-C₃ and C₄-H), 7.34 (dd, 2H, pyrrole-C₂ and C₅-H), 7.83 (d, 2H, *J* = 8 Hz, Ph-C₃ and C₅-H), 8.11 (d, 2H, *J* = 10 Hz, Ph-C₂ and C₆-H), 11.33 (s, 1H, amide-NH); ¹³C NMR (400 MHz, DMSO-*d*₆) δ ppm: 167.81 (amide-C=O), 165.33 (isoindoline-C₁ and C₃), 145.39 (Ph-C₄), 137.05 (isoindoline-C₅ and C₆), 135.60 (isoindoline-C₈ and C₉), 130.21 (Ph-C₃ and C₅), 129.11 (isoindoline-C₄ and C₇), 128.57 (Ph-C₁), 127.22 (Ph-C₂ and C₆), 122.01 (pyrrole-C₂ and C₅), 111.89 (pyrrole-C₃ and C₄); MS (ESI): *m/z* = found 468.94 [M⁺], 466.94 [M⁺-2], 470.93 [M⁺+2], 402/400, 300/298, 286/284, 186, 170, 142, 120, 67; calcd. 469.11. Anal. C₁₉H₉Cl₄N₃O₃.

4-(1*H*-pyrrol-1-yl)-*N*-(4,5,6,7-tetrafluoro-1,3-dioxoisindolin-2-yl)benzamide (**5h**) Yield 43 %. mp 260–262 °C; FTIR (KBr): 3230 (NH), 3222, 2911 (Ar-H), 1785 (isoindoline C=O), 1749 (isoindoline C=O), 1691 (amide C=O) cm⁻¹; ¹H NMR (400 MHz, DMSO-*d*₆) δ ppm: 6.43 (dd, 2H, pyrrole-C₃ and C₄-H), 7.39 (dd, 2H, pyrrole-C₂ and C₅-H), 7.87 (d, 2H, *J* = 8 Hz, Ph-C₃ and C₅-H), 8.13 (d, 2H, *J* = 8 Hz, Ph-C₂ and C₆-H), 13.01 (s, 1H, amide-NH); ¹³C NMR (400 MHz, DMSO-*d*₆) δ ppm: 167.93 (amide-C=O), 166.01 (isoindoline-C₁ and C₃), 144.58

(Ph–C₄), 143.60 (isoindoline–C₅ and C₆), 142.81 (isoindoline–C₄ and C₇), 130.61 (Ph–C₃ and C₅), 128.80 (Ph–C₁), 128.56 (Ph–C₂ and C₆), 122.19 (pyrrole–C₂ and C₅), 120.09 (isoindoline–C₈ and C₉), 111.30 (pyrrole–C₃ and C₄); MS (ESI): m/z = found 403.06 [M⁺], 338, 218, 186, 142, 120, 105, 67; calcd. 403.29. Anal. C₁₉H₉F₄N₃O₃.

N-(5,6-dichloro-1,3-dioxoisindolin-2-yl)-4-(1*H*-pyrrol-1-yl)benzamide (**5i**) Yield 51 %. mp 254–256 °C; FTIR (KBr): 3223 (NH), 2993, 2955 (Ar–H), 1777 (isoindoline C=O), 1745 (isoindoline C=O), 1687 (amide C=O) cm⁻¹; ¹H NMR (400 MHz, DMSO-*d*₆) δ ppm: 6.33 (dd, 2H, pyrrole–C₃ and C₄–H), 7.47 (dd, 2H, pyrrole–C₂ and C₅–H), 7.68 (d, 2H, *J* = 8 Hz, Ph–C₃ and C₅–H), 8.03 (d, 2H, *J* = 8.5 Hz, Ph–C₂ and C₆–H), 8.15 (d, 2H, isoindoline–C₄ and C₇–H), 12.27 (s, 1H, amide–NH); ¹³C NMR (400 MHz, DMSO-*d*₆) δ ppm: 169.80 (amide–C=O), 165.89 (isoindoline–C₁ and C₃), 141.89 (Ph–C₄), 135.29 (isoindoline–C₅ and C₆), 133.21 (isoindoline–C₈ and C₉), 130.30 (Ph–C₃ and C₅), 129.57 (isoindoline–C₄ and C₇), 128.30 (Ph–C₁), 128.01 (Ph–C₂ and C₆), 119.70 (pyrrole–C₂ and C₅), 110.89 (pyrrole–C₃ and C₄); MS (ESI): m/z = found 400.02 [M⁺], 401.01 [M⁺+1], 402.02 [M⁺+2], 334/332, 230/232, 215/213, 186, 142, 120, 67; calcd. 400.21. Anal. C₁₉H₁₁Cl₂N₃O₃.

N-(5-methyl-1,3-dioxoisindolin-2-yl)-4-(1*H*-pyrrol-1-yl)benzamide (**5j**) Yield 60 %. mp 240–242 °C; FTIR (KBr): 3230 (NH), 3011, 2988 (Ar–H), 1781 (isoindoline C=O), 1749 (isoindoline C=O), 1680 (amide C=O) cm⁻¹; ¹H NMR (400 MHz, DMSO-*d*₆) δ ppm: 2.51 (s, 3H, isoindoline–5-CH₃), 6.40 (dd, 2H, pyrrole–C₃ and C₄–H), 7.30 (dd, 2H, pyrrole–C₂ and C₅–H), 7.56–7.77 (m, 3H, Ph–C₃, C₅–H and isoindoline–C₆–H), 7.83–8.01 (m, 2H, isoindoline–C₄ and C₇–H), 8.20 (d, 2H, *J* = 10 Hz, Ph–C₂ and C₆–H), 11.29 (s, 1H, amide–NH); ¹³C NMR (400 MHz, DMSO-*d*₆) δ ppm: 168.01 (amide–C=O), 165.73 (isoindoline–C₁ and C₃), 142.23 (Ph–C₄), 141.83 (isoindoline–C₅), 133.19 (isoindoline–C₆), 132.30 (isoindoline–C₉), 130.13 (Ph–C₃ and C₅), 129.81 (isoindoline–C₈), 125.88 (Ph–C₁), 125.33 (Ph–C₂ and C₆), 124.55 (isoindoline–C₄ and C₇), 120.66 (pyrrole–C₂ and C₅), 111.37 (pyrrole–C₃ and C₄), 22.13 (isoindoline–5-CH₃); MS (ESI): m/z = found 345.11 [M⁺], 280, 200, 186, 176, 170, 160, 146, 67; calcd. 345.35. Anal. C₂₀H₁₅N₃O₃.

N-(5-nitro-1,3-dioxoisindolin-2-yl)-4-(1*H*-pyrrol-1-yl)benzamide (**5k**) Yield 40 %. mp 270–272 °C; FTIR (KBr): 3241 (NH), 3217, 2971 (Ar–H), 1732 (isoindoline C=O), 1701 (isoindoline C=O), 1636 (amide C=O) cm⁻¹; ¹H NMR (400 MHz, DMSO-*d*₆) δ ppm: 6.17 (dd, 2H, pyrrole–C₃ and C₄–H), 7.20 (dd, 2H, pyrrole–C₂ and C₅–H), 7.59 (d, 2H, *J* = 8.5 Hz, Ph–C₃ and C₅–H), 8.01 (d,

2H, *J* = 8.5 Hz, Ph–C₂ and C₆–H), 8.15–8.70 (m, 3H, isoindoline–C₄, C₆ and C₇–H), 12.09 (s, 1H, amide–NH); ¹³C NMR (400 MHz, DMSO-*d*₆) δ ppm: 170.09 (amide–C=O), 167.13 (isoindoline–C₁ and C₃), 155.03 (isoindoline–C₅), 145.21 (Ph–C₄), 140.11 (isoindoline–C₈), 133.90 (isoindoline–C₉), 131.09 (Ph–C₃ and C₅), 130.11 (isoindoline–C₇), 129.03 (Ph–C₂ and C₆), 128.88 (Ph–C₁), 128.05 (isoindoline–C₆), 122.29 (isoindoline–C₄), 118.05 (pyrrole–C₂ and C₅), 111.89 (pyrrole–C₃ and C₄); MS (ESI): m/z = found 376.08 [M⁺], 266, 207, 191, 186, 170, 167, 146, 67; calcd. 376.32. Anal. C₁₉H₁₂N₄O₅.

4-(1*H*-pyrrol-1-yl)-*N*-(4-nitro-1,3-dioxoisindolin-2-yl)benzamide (**5l**) Yield 40 %. mp 252–254 °C; FTIR (KBr): 3255 (NH), 3001, 2976 (Ar–H), 1750 (isoindoline C=O), 1713 (isoindoline C=O), 1651 (amide C=O) cm⁻¹; ¹H NMR (400 MHz, DMSO-*d*₆) δ ppm: 6.20 (dd, 2H, pyrrole–C₃ and C₄–H), 7.35 (dd, 2H, pyrrole–C₂ and C₅–H), 7.83 (d, 2H, *J* = 8 Hz, Ph–C₃ and C₅–H), 8.29 (d, 2H, *J* = 8 Hz, Ph–C₂ and C₆–H), 8.35–8.76 (m, 3H, isoindoline–C₅, C₆ and C₇–H), 13.01 (s, 1H, amide–NH); ¹³C NMR (400 MHz, DMSO-*d*₆) δ ppm: 169.70 (amide–C=O), 167.80 (isoindoline–C₁ and C₃), 149.21 (isoindoline–C₄), 145.03 (Ph–C₄), 135.29 (isoindoline–C₆), 134.70 (isoindoline–C₈), 130.23 (isoindoline–C₇), 129.08 (Ph–C₃ and C₅), 128.88 (Ph–C₁, C₂ and C₆), 128.03 (isoindoline–C₅ and C₉), 121.05 (pyrrole–C₂ and C₅), 111.57 (pyrrole–C₃ and C₄); MS (ESI): m/z = found 376.08 [M⁺], 311, 207, 191, 186, 170, 167, 146, 67; calcd. 376.32. Anal. C₁₉H₁₂N₄O₅.

N-(1,3-dioxohexahydro-1*H*-isoindol-2(3*H*)-yl)-4-(1*H*-pyrrol-1-yl)benzamide (**5m**) Yield 57 %. mp 228–230 °C; FTIR (KBr): 3241 (NH), 2999, 2956 (Ar–H), 1729 (isoindoline C=O), 1699 (isoindoline C=O), 1629 (amide C=O) cm⁻¹; ¹H NMR (400 MHz, DMSO-*d*₆) δ ppm: 1.40–1.52 (m, 4H, isoindoline–C₅ and C₆–H), 1.55–1.79 (m, 4H, isoindoline–C₄ and C₇–H), 2.57 (d, 2H, isoindoline–C₈ and C₉–H), 6.13 (dd, 2H, pyrrole–C₃ and C₄–H), 7.31 (dd, 2H, pyrrole–C₂ and C₅–H), 7.51 (d, 2H, *J* = 8 Hz, Ph–C₃ and C₅–H), 8.01 (d, 2H, *J* = 8 Hz, Ph–C₂ and C₆–H), 11.33 (s, 1H, amide–NH); ¹³C NMR (400 MHz, DMSO-*d*₆) δ ppm: 176.01 (isoindoline–C₃), 167.09 (amide–C=O), 145.01 (Ph–C₄), 130.05 (Ph–C₃ and C₅), 129.08 (Ph–C₁), 128.81 (Ph–C₂ and C₆), 120.40 (pyrrole–C₂ and C₅), 111.01 (pyrrole–C₃ and C₄), 40.11 (isoindoline–C₈ and C₉), 28.09 (isoindoline–C₄ and C₇), 26.03 (isoindoline–C₅ and C₆); MS (ESI): m/z = found 337.14 [M⁺], 271, 186, 170, 168, 152, 120, 67; calcd. 337.37. Anal. C₁₉H₁₉N₃O₃.

Synthesis of ethyl 4-(2,5-dimethylpyrrol-1-yl)benzoate (**6**)

A mixture of acetyl acetone (13.69 g, 120 mmol) and ethyl 4-aminobenzoate (**2**; 16.5 g, 100 mmol) in glacial

acetic acid (100 mL) was refluxed for 1 h. The solvent was removed under reduced pressure, residue thus obtained was collected by filtration, washed with water, dried, and recrystallized from ethanol (yield 65 %). mp 87–88 °C (Joshi *et al.*, 2013a).

Synthesis of 4-(2,5-dimethylpyrrol-1-yl)benzoic acid hydrazide (7)

Compound **2** was synthesized by refluxing a mixture of ethyl 4-(2,5-dimethylpyrrol-1-yl)benzoate (**1**; 3.64 g, 15 mmol) with hydrazine hydrate (10 mL) in absolute ethanol (10 mL) for 3 h (monitored by TLC). The cooled mixture was poured gradually onto crushed ice cubes with stirring. The mixture was allowed to stand and solid was separated. It was filtered, washed thoroughly with cold water, dried, and recrystallized from ethanol (yield 80 %). mp 170–172 °C (Joshi *et al.*, 2013a).

General procedure for the preparation of N-(substituted)-4-(2,5-dimethyl-1H-pyrrol-1-yl)benzamides (8a–m)

Mixture of 4-(2,5-dimethyl-1H-pyrrol-1-yl)benzohydrazide (25 mmol) and anhydride (25 mmol) in 10 mL dried acetic acid was stirred for 30 min at room temperature. The separated solid was filtered, washed with diethyl ether, and dried. The solid was dissolved in 30 mL dried acetic acid and stirred overnight under nitrogen atmosphere. The reaction mixture was then poured into ice-cold water; the separated solid was collected, washed with water, dried, and recrystallized by aqueous methanol/DMF to get the desired product **8a–m**.

4-(2,5-Dimethyl-1H-pyrrol-1-yl)-N-(2,5-dioxo-2,5-dihydro-1H-pyrrol-1-yl)benzamide (8a) Yield 40 %. mp 254–256 °C; FTIR (KBr): 3239 (NH), 3019, 2985 (Ar–H), 1750 (2,5-dihydropyrrole C=O), 1673 (amide C=O) cm^{-1} ; ^1H NMR (500 MHz, DMSO- d_6) δ ppm: 1.99 (s, 6H, 2CH₃), 5.85 (dd, 2H, pyrrole–C₃ and C₄–H), 7.79 (d, 2H, $J = 8$ Hz, Ph–C₃ and C₅–H), 8.01 (d, 2H, $J = 8$ Hz, Ph–C₂ and C₆–H), 9.29 (s, 2H, 2,5-dihydropyrrole–C₃ and C₄–H), 11.29 (s, 1H, amide–NH); ^{13}C NMR (500 MHz, DMSO- d_6) δ ppm: 165.21 (amide–C=O), 164.81 (2,5-dihydropyrrole–C₂), 164.33 (2,5-dihydropyrrole–C₅), 143.21 (Ph–C₄), 138.29 (2,5-dihydropyrrole–C₃ and C₄), 131.20 (Ph–C₃ and C₅), 129.21 (Ph–C₁), 128.91 (Ph–C₂ and C₆), 127.35 (pyrrole–C₂ and C₅), 106.01 (pyrrole–C₃ and C₄), 11.99 (pyrrole–2CH₃); MS (ESI): $m/z =$ found 309.11 [M^+], 283, 256, 216, 171, 139, 112, 96; calcd. 309.32. Anal. C₁₇H₁₅N₃O₃.

4-(2,5-Dimethyl-1H-pyrrol-1-yl)-N-(2,5-dioxopyrrolidin-1-yl)benzamide (8b) Yield 39 %. mp 190–192 °C; FTIR

(KBr): 3251 (NH), 3022, 2931 (Ar–H), 1745 (pyrrolidine C=O), 1681 (amide C=O) cm^{-1} ; ^1H NMR (500 MHz, DMSO- d_6) δ ppm: 2.03 (s, 6H, 2CH₃), 2.49–2.58 (m, 4H, pyrrolidine–C₃ and C₄–H), 5.81 (dd, 2H, pyrrole–C₃ and C₄–H), 7.69 (d, 2H, $J = 7.5$ Hz, Ph–C₃ and C₅–H), 7.99 (d, 2H, $J = 8$ Hz, Ph–C₂ and C₆–H), 10.59 (s, 1H, amide–NH); ^{13}C NMR (500 MHz, DMSO- d_6) δ ppm: 170.29 (pyrrolidine–C₂ and C₅), 165.29 (amide–C=O), 142.23 (Ph–C₄), 130.33 (Ph–C₃ and C₅), 128.81 (Ph–C₁), 128.55 (Ph–C₂ and C₆), 127.49 (pyrrole–C₂ and C₅), 105.87 (pyrrole–C₃ and C₄), 29.71 (pyrrolidine–C₃ and C₄), 12.70 (pyrrole–2CH₃); MS (ESI): $m/z =$ found 311.13 [M^+], 283, 256, 218, 198, 141, 114, 98; calcd. 311.34. Anal. C₁₇H₁₇N₃O₃.

4-(2,5-Dimethyl-1H-pyrrol-1-yl)-N-(3-methyl-2,5-dioxo-2,5-dihydro-1H-pyrrol-1-yl)benzamide (8c) Yield 60 %. mp 208–210 °C; FTIR (KBr): 3267 (NH), 3087, 2919 (Ar–H), 1738 (pyrrole C=O), 1661 (amide C=O) cm^{-1} ; ^1H NMR (400 MHz, CDCl₃) δ ppm: 1.96 (s, 6H, 2CH₃), 2.10 (s, 3H, CH₃ at 2,5-dihydropyrrole–C₃), 5.79 (s, 2H, pyrrole–C₃ and C₄–H), 6.71 (s, 1H, 2,5-dihydropyrrole–C₃–H), 7.36 (d, 2H, $J = 8$ Hz, Ph–C₃ and C₅–H), 8.05 (d, 2H, $J = 8$ Hz, Ph–C₂ and C₆–H), 11.05 (s, 1H, amide–NH); ^{13}C NMR (400 MHz, CDCl₃) δ ppm: 168.72 (amide–C=O), 167.64 (2,5-dihydropyrrole–C₂), 164.49 (2,5-dihydropyrrole–C₅), 144.62 (2,5-dihydropyrrole–C₃), 142.03 (Ph–C₄), 130.67 (Ph–C₃ and C₅), 129.74 (Ph–C₂ and C₆), 127.79 (2,5-dihydropyrrole–C₄), 127.52 (Ph–C₁), 126.62 (pyrrole–C₂ and C₅), 106.35 (pyrrole–C₃ and C₄), 12.74 (CH₃ of 2,5-dihydropyrrole–C₃), 11.07 (pyrrole–2CH₃); MS (ESI): $m/z =$ found 323.13 [M^+], 230, 171, 153, 126, 112, 110, 96; calcd. 323.35. Anal. C₁₈H₁₇N₃O₃.

4-(2,5-Dimethyl-1H-pyrrol-1-yl)-N-(3-methylene-2,5-dioxopyrrolidin-1-yl)benzamide (8d) Yield 52 %. mp 184–186 °C; FTIR (KBr): 3221 (NH), 3022, 2923 (Ar–H), 1693 (pyrrolidine C=O), 1636 (amide C=O) cm^{-1} ; ^1H NMR (400 MHz, DMSO- d_6) δ ppm: 2.01 (s, 6H, 2CH₃), 5.82 (s, 2H, CH₂ at pyrrolidine–C₃), 6.21 (s, 2H, CH₂ at pyrrolidine–C₄), 6.26 (s, 2H, pyrrole–C₃ and C₄–H), 7.30 (d, 2H, $J = 8.4$ Hz, Ph–C₃ and C₅–H), 8.08 (d, 2H, $J = 8.4$ Hz, Ph–C₂ and C₆–H), 10.00 (s, 1H, amide–NH); ^{13}C NMR (400 MHz, DMSO- d_6) δ ppm: 168.86 (amide–C=O), 167.58 (pyrrolidine–C₂), 164.76 (pyrrolidine–C₅), 141.26 (Ph–C₄), 134.78 (pyrrolidine–C₃), 131.29 (CH₂ at pyrrolidine–C₃), 128.35 (Ph–C₃ and C₅), 127.65 (Ph–C₁), 127.45 (Ph–C₂ and C₆), 127.26 (pyrrole–C₂ and C₅), 106.00 (pyrrole–C₃ and C₄), 36.60 (pyrrolidine–C₄), 12.68 (pyrrole–2CH₃); MS (ESI): $m/z =$ found 323.13 [M^+], 283, 256, 230, 198, 126, 110, 98, 95; calcd. 323.35. Anal. C₁₈H₁₇N₃O₃.

4-(2,5-Dimethyl-1H-pyrrol-1-yl)-N-(1,3-dioxoisindolin-2-yl)benzamide (8e) Yield 79 %. mp 196–198 °C; FTIR (KBr): 3246 (NH), 3017, 2913 (Ar–H), 1705 (isoindoline C=O), 1667 (amide C=O) cm^{-1} ; ^1H NMR (400 MHz, DMSO- d_6) δ ppm: 2.02 (s, 6H, 2CH₃), 5.83 (s, 2H, pyrrole–C₃ and C₄–H), 7.29 (d, 2H, $J = 8.24$ Hz, Ph–C₃ and C₅–H), 7.50–7.94 (m, 4H, isoindoline–C₄, C₅, C₆ and C₇–H), 8.17 (d, 2H, $J = 8$ Hz, Ph–C₂ and C₆–H), 10.70 (s, 1H, amide–NH); ^{13}C NMR (500 MHz, CDCl₃) δ ppm: 168.11 (amide–C=O), 164.91 (isoindoline–C₃), 159.93 (isoindoline–C₁), 141.32 (Ph–C₄), 135.97 (isoindoline–C₅ and C₆), 132.19 (isoindoline–C₉), 131.30 (isoindoline–C₈), 129.37 (Ph–C₃ and C₅), 128.54 (Ph–C₁), 128.26 (Ph–C₂ and C₆), 127.59 (pyrrole–C₂ and C₅), 127.47 (isoindoline–C₄ and C₇), 106.11 (pyrrole–C₃ and C₄), 12.71 (pyrrole–2CH₃); MS (ESI): $m/z =$ found 359.13 [M^+], 283, 266, 256, 214, 198, 171, 162, 146, 95; calcd. 359.38. Anal. C₂₁H₁₇N₃O₃.

4-(2,5-Dimethyl-1H-pyrrol-1-yl)-N-(4,5,6,7-tetrabromo-1,3-dioxoisindolin-2-yl)benzamide (8f) Yield 53 %. mp >300 °C; FTIR (KBr): 3237 (NH), 2976, 2919 (Ar–H), 1744 (isoindoline C=O), 1699 (amide C=O), 1651 (isoindoline C=O) cm^{-1} ; ^1H NMR (400 MHz, DMSO- d_6) δ ppm: 2.05 (s, 6H, 2CH₃), 5.85 (s, 2H, pyrrole–C₃ and C₄–H), 7.40 (d, 2H, $J = 8.48$ Hz, Ph–C₃ and C₅–H), 8.16 (d, 2H, $J = 8.52$ Hz, Ph–C₂ and C₆–H), 11.47 (s, 1H, amide–NH); ^{13}C NMR (400 MHz, DMSO- d_6) δ ppm: 160.85 (amide–C=O), 160.31 (isoindoline–C₁ and C₃), 142.24 (Ph–C₄), 137.66 (isoindoline–C₈ and C₉), 128.88 (isoindoline–C₅ and C₆), 128.72 (Ph–C₃ and C₅), 127.84 (Ph–C₁, C₂ and C₆), 127.55 (pyrrole–C₂ and C₅), 121.37 (isoindoline–C₄ and C₇), 106.39 (pyrrole–C₃ and C₄), 12.76 (pyrrole–2CH₃); MS (ESI): $m/z =$ found 674.76 [M^+], 672.77 [$\text{M}^+ - 2$], 676.76 [$\text{M}^+ + 2$], 582/580, 476/474, 462/460, 283, 256, 214, 198, 171, 95; calcd. 674.96. Anal. C₂₁H₁₃Br₄N₃O₃.

4-(2,5-Dimethyl-1H-pyrrol-1-yl)-N-(4,5,6,7-tetrachloro-1,3-dioxoisindolin-2-yl)benzamide (8g) Yield 57 %. mp >300 °C; FTIR (KBr): 3255 (NH), 3018, 2928 (Ar–H), 1740 (isoindoline C=O), 1696 (isoindoline C=O), 1650 (amide C=O) cm^{-1} ; ^1H NMR (400 MHz, DMSO- d_6) δ ppm: 2.03 (s, 6H, 2CH₃), 5.87 (dd, 2H, pyrrole–C₃ and C₄–H), 7.77 (d, 2H, $J = 8$ Hz, Ph–C₃ and C₅–H), 8.09 (d, 2H, $J = 8$ Hz, Ph–C₂ and C₆–H), 10.89 (s, 1H, amide–NH); ^{13}C NMR (400 MHz, DMSO- d_6) δ ppm: 165.27 (amide–C=O), 164.59 (isoindoline–C₁ and C₃), 143.55 (Ph–C₄), 140.11 (isoindoline–C₅ and C₆), 135.29 (isoindoline–C₈ and C₉), 130.91 (isoindoline–C₄ and C₇), 128.11 (Ph–C₃ and C₅), 128.01 (Ph–C₁), 127.81 (Ph–C₂ and C₆), 127.35 (pyrrole–C₂ and C₅), 106.17 (pyrrole–C₃ and C₄), 12.31 (pyrrole–2CH₃); MS (ESI): $m/z =$ found 496.97 [M^+], 494.97 [$\text{M}^+ - 2$], 498.97 [$\text{M}^+ + 2$], 404/402, 300/298, 286/

284, 299, 284, 266, 214, 198, 171, 95; calcd. 497.16. Anal. C₂₁H₁₃Cl₄N₃O₃.

4-(2,5-Dimethyl-1H-pyrrol-1-yl)-N-(4,5,6,7-tetrafluoro-1,3-dioxoisindolin-2-yl)benzamide (8h) Yield 40 %. mp 284–286 °C; FTIR (KBr): 3243 (NH), 2987, 2930 (Ar–H), 1751 (isoindoline C=O), 1676 (isoindoline C=O), 1641 (amide C=O) cm^{-1} ; ^1H NMR (400 MHz, DMSO- d_6) δ ppm: 2.10 (s, 6H, 2CH₃), 5.89 (dd, 2H, pyrrole–C₃ and C₄–H), 7.83 (d, 2H, $J = 8$ Hz, Ph–C₃ and C₅–H), 8.11 (d, 2H, $J = 10$ Hz, Ph–C₂ and C₆–H), 11.12 (s, 1H, amide–NH); ^{13}C NMR (400 MHz, DMSO- d_6) δ ppm: 167.11 (amide–C=O), 165.71 (isoindoline–C₁ and C₃), 145.71 (isoindoline–C₅ and C₆), 145.01 (isoindoline–C₄ and C₇), 143.71 (Ph–C₄), 131.22 (Ph–C₃ and C₅), 129.11 (Ph–C₁, C₂ and C₆), 128.71 (pyrrole–C₂ and C₅), 119.09 (isoindoline–C₈ and C₉), 107.11 (pyrrole–C₃ and C₄), 12.70 (pyrrole–2CH₃); MS (ESI): $m/z =$ found 431.09 [M^+], 338, 234, 218, 214, 198, 176, 171, 95; calcd. 431.34. Anal. C₂₁H₁₃F₄N₃O₃.

N-(5,6-dichloro-1,3-dioxoisindolin-2-yl)-4-(2,5-dimethyl-1H-pyrrol-1-yl)benzamide (8i) Yield 49 %. mp 274–276 °C; FTIR (KBr): 3220 (NH), 2999, 2945 (Ar–H), 1759 (isoindoline C=O), 1681 (isoindoline C=O), 1637 (amide C=O) cm^{-1} ; ^1H NMR (400 MHz, DMSO- d_6) δ ppm: 2.01 (s, 6H, 2CH₃), 5.81 (dd, 2H, pyrrole–C₃ and C₄–H), 7.81 (d, 2H, $J = 8.5$ Hz, Ph–C₃ and C₅–H), 8.09 (d, 2H, $J = 8.5$ Hz, Ph–C₂ and C₆–H), 8.09 (d, 2H, isoindoline–C₄ and C₇–H), 11.87 (s, 1H, amide–NH); ^{13}C NMR (400 MHz, DMSO- d_6) δ ppm: 170.23 (amide–C=O), 167.31 (isoindoline–C₁ and C₃), 144.22 (Ph–C₄), 140.21 (isoindoline–C₅ and C₆), 135.21 (isoindoline–C₈ and C₉), 130.51 (Ph–C₃ and C₅), 129.85 (isoindoline–C₄ and C₇), 129.23 (Ph–C₁), 128.83 (Ph–C₂ and C₆), 127.15 (pyrrole–C₂ and C₅), 106.50 (pyrrole–C₃ and C₄), 12.75 (pyrrole–2CH₃); MS (ESI): $m/z =$ found 428.05 [M^+], 430.05 [$\text{M}^+ + 2$], 334/332, 258/256, 232/230, 215, 214, 198, 171, 95; calcd. 428.27. Anal. C₂₁H₁₅Cl₂N₃O₃.

4-(2,5-Dimethyl-1H-pyrrol-1-yl)-N-(5-methyl-1,3-dioxoisindolin-2-yl)benzamide (8j) Yield 65 %. mp 192–194 °C; FTIR (KBr): 3257 (NH), 3021, 2977 (Ar–H), 1746 (isoindoline C=O), 1693 (isoindoline C=O), 1650 (amide C=O) cm^{-1} ; ^1H NMR (400 MHz, DMSO- d_6) δ ppm: 1.96 (s, 6H, 2CH₃), 2.30 (s, 3H, isoindoline–5-CH₃), 5.81 (dd, 2H, pyrrole–C₃ and C₄–H), 7.66–7.79 (m, 3H, Ph–C₃, C₅–H and isoindoline–C₆–H), 7.89–7.98 (m, 2H, isoindoline–C₄ and C₇–H), 8.01 (d, 2H, $J = 8.5$ Hz, Ph–C₂ and C₆–H), 12.01 (s, 1H, amide–NH); ^{13}C NMR (400 MHz, DMSO- d_6) δ ppm: 170.20 (amide–C=O), 167.33 (isoindoline–C₁ and C₃), 142.11 (Ph–C₄), 141.81 (isoindoline–C₅), 133.45 (isoindoline–C₆), 132.21 (isoindoline–C₉), 130.27 (Ph–C₃

and C₅), 129.73 (isoindoline–C₈), 128.39 (Ph–C₁), 128.11 (Ph–C₂ and C₆), 127.81 (pyrrole–C₂ and C₅), 126.58 (isoindoline–C₄ and C₇), 106.28 (pyrrole–C₃ and C₄), 22.01 (isoindoline–5-CH₃), 12.71 (pyrrole–2CH₃); MS (ESI): *m/z* = found 373.14 [M⁺], 280, 214, 198, 176, 171, 162, 160, 146, 95; calcd. 373.40. Anal. C₂₂H₁₉N₃O₃.

4-(2,5-Dimethyl-1H-pyrrol-1-yl)-N-(5-nitro-1,3-dioxoisoindolin-2-yl)benzamide (8k) Yield 39 %. mp 188–190 °C; FTIR (KBr): 3249 (NH), 3003, 2954 (Ar–H), 1723 (isoindoline C=O), 1654 (isoindoline C=O), 1605 (amide C=O) cm⁻¹; ¹H NMR (400 MHz, DMSO-*d*₆) δ ppm: 2.03 (s, 6H, 2CH₃), 5.89 (dd, 2H, pyrrole–C₃ and C₄–H), 7.57 (d, 2H, *J* = 8 Hz, Ph–C₃ and C₅–H), 8.11 (d, 2H, *J* = 8 Hz, Ph–C₂ and C₆–H), 8.15–8.70 (m, 3H, isoindoline–C₄, C₆ and C₇–H), 12.63 (s, 1H, amide–NH); ¹³C NMR (400 MHz, DMSO-*d*₆) δ ppm: 168.35 (amide–C=O), 165.29 (isoindoline–C₁ and C₃), 155.27 (isoindoline–C₅), 143.33 (Ph–C₄), 140.29 (isoindoline–C₈), 139.87 (isoindoline–C₉), 133.21 (Ph–C₃ and C₅), 128.85 (isoindoline–C₇ and Ph–C₁), 128.55 (Ph–C₂ and C₆), 128.20 (pyrrole–C₂ and C₅), 127.31 (isoindoline–C₆), 123.29 (isoindoline–C₄), 105.91 (pyrrole–C₃ and C₄), 12.30 (pyrrole–2CH₃); MS (ESI): *m/z* = found 404.11 [M⁺], 311, 214, 198, 191, 171, 162, 146, 95; calcd. 404.38. Anal. C₂₁H₁₆N₄O₅.

4-(2,5-Dimethyl-1H-pyrrol-1-yl)-N-(4-nitro-1,3-dioxoisoindolin-2-yl)benzamide (8l) Yield 39 %. mp 158–160 °C; FTIR (KBr): 3271 (NH), 2989, 2933 (Ar–H), 1742 (isoindoline C=O), 1644 (isoindoline C=O), 1615 (amide C=O) cm⁻¹; ¹H NMR (400 MHz, DMSO-*d*₆) δ ppm: 2.07 (s, 6H, 2CH₃), 5.77 (dd, 2H, pyrrole–C₃ and C₄–H), 7.69 (d, 2H, *J* = 8 Hz, Ph–C₃ and C₅–H), 7.99 (d, 2H, *J* = 10 Hz, Ph–C₂ and C₆–H), 8.15–8.65 (m, 3H, isoindoline–C₅, C₆ and C₇–H), 10.90 (s, 1H, amide–NH); ¹³C NMR (400 MHz, DMSO-*d*₆) δ ppm: 169.23 (amide–C=O), 167.30 (isoindoline–C₁ and C₃), 147.23 (isoindoline–C₄), 144.81 (Ph–C₄), 135.23 (isoindoline–C₆), 134.29 (isoindoline–C₈), 130.25 (isoindoline–C₇), 129.35 (Ph–C₃ and C₅), 128.76 (Ph–C₁, C₂ and C₆), 128.55 (isoindoline–C₅ and C₉), 128.31 (pyrrole–C₂ and C₅), 106.21 (pyrrole–C₃ and C₄), 12.35 (pyrrole–2CH₃); MS (ESI): *m/z* = found 404.11 [M⁺], 311, 266, 214, 198, 191, 171, 162, 149, 146, 95; calcd. 404.38. Anal. C₂₁H₁₆N₄O₅.

4-(2,5-Dimethyl-1H-pyrrol-1-yl)-N-(1,3-dioxohexahydro-1H-isoindol-2(3H)-yl)benzamide (8m) Yield 59 %. mp 206–208 °C; FTIR (KBr): 3231 (NH), 3020, 2954 (Ar–H), 1709 (isoindoline C=O), 1651 (isoindoline C=O), 1610 (amide C=O) cm⁻¹; ¹H NMR (400 MHz, DMSO-*d*₆) δ ppm: 1.45–1.52 (m, 4H, isoindoline–C₅ and C₆–H), 1.56–1.80 (m, 4H, isoindoline–C₄ and C₇–H), 2.04 (s, 6H, 2CH₃), 2.53 (d, 2H, isoindoline–C₈ and C₉–H), 5.80 (dd,

2H, pyrrole–C₃ and C₄–H), 7.73 (d, 2H, *J* = 8.5 Hz, Ph–C₃ and C₅–H), 8.09 (d, 2H, *J* = 8.5 Hz, Ph–C₂ and C₆–H), 10.95 (s, 1H, amide–NH); ¹³C NMR (400 MHz, DMSO-*d*₆) δ ppm: 176.10 (isoindoline–C₃), 167.21 (amide–C=O), 145.27 (Ph–C₄), 130.21 (Ph–C₃ and C₅), 129.31 (Ph–C₁, C₂ and C₆), 129.01 (pyrrole–C₂ and C₅), 105.90 (pyrrole–C₃ and C₄), 40.22 (isoindoline–C₈ and C₉), 29.01 (isoindoline–C₄ and C₇), 26.33 (isoindoline–C₅ and C₆), 12.29 (pyrrole–2CH₃); MS (ESI): *m/z* = found 365.17 [M⁺], 271, 256, 214, 198, 171, 168, 152, 110, 95; calcd. 365.43. Anal. C₂₁H₂₃N₃O₃.

General procedure for the preparation of 2-amino-4-(4-substituted phenyl)thiazoles (11a–l)

Mixture of substituted acetophenone (100 mmol), thiourea (200 mmol), and iodine or bromine (100 mmol) was refluxed for 24 h on a water bath. The reaction mixture was cooled, washed with ether, added to boiling water, and filtered while hot. The filtrate was cooled and basified with ammonium hydroxide solution. The crude product obtained was filtered, dried, and recrystallized from aqueous ethanol to get the desired product (11a–l; Pattan *et al.*, 2006; Dickey *et al.*, 1959; Singh *et al.*, 2010).

General procedure for the preparation of 4-(4-substituted phenyl)-2-(1H-pyrrol-1-yl)thiazoles (12a–l)

To a solution of 2-amino-4-(4-substituted phenyl)thiazoles (10 mmol) in 20 mL glacial acetic acid, 2,5-dimethoxytetrahydrofuran (15 mmol) was added slowly at room temperature and was refluxed for 1 h (monitored by TLC). The reaction mixture was poured into ice-cold water and basified with ammonium carbonate solution. The separated solid was collected, washed with water, and dried. The compounds were purified by column chromatography using chromatotron (hexane/ethyl acetate 70:30).

4-Phenyl-2-(1H-pyrrol-1-yl)thiazole (12a) Yield 71 %. mp 59–61 °C; FTIR (KBr): 2921 and 2851 (Ar–H), 1599 (C=N) cm⁻¹; ¹H NMR (500 MHz, CDCl₃) δ ppm: 6.39 (s, 2H, pyrrole–C₃ and C₄–H), 7.15 (s, 1H, thiazole–C₅–H), 7.36–7.50 (m, 5H, Ph–C₃, C₄ and C₅–H, pyrrole–C₂ and C₅–H), 7.95 (d, 2H, *J* = 7.5 Hz, Ph–C₂ and C₆–H); ¹³C NMR (500 MHz, CDCl₃) δ ppm: 159.76 (thiazole–C₂), 152.44 (thiazole–C₄), 127.54 (Ph–C₂ and C₆), 127.08 (Ph–C₃ and C₅), 119.67 (Ph–C₁ and C₄), 114.09 (pyrrole–C₂ and C₅), 111.84 (pyrrole–C₃ and C₄), 105.00 (thiazole–C₅); MS (ESI): *m/z* = found 226.06 [M⁺], 150, 119, 85; calcd. 226.30. Anal. C₁₃H₁₀N₂S.

4-(4-Chlorophenyl)-2-(1H-pyrrol-1-yl)thiazole (12b) Yield 89 %. mp 64–66 °C; FTIR (KBr): 2971 and 2937 (Ar–H),

1595 (C=N) cm^{-1} ; ^1H NMR (400 MHz, CDCl_3) δ ppm: 6.32 (dd, 2H, pyrrole- C_3 and C_4 -H), 6.80–6.98 (m, 2H, Ph- C_3 and C_5 -H), 7.12 (s, 1H, thiazole- C_5 -H), 7.48 (dd, 2H, pyrrole- C_2 and C_5 -H), 7.81–7.92 (m, 2H, Ph- C_2 and C_6 -H); ^{13}C NMR (400 MHz, CDCl_3) δ ppm: 159.69 (thiazole- C_2), 158.56 (Ph- C_4), 153.24 (thiazole- C_4), 127.26 (Ph- C_2 and C_6), 125.85 (Ph- C_1), 119.98 (pyrrole- C_2 and C_5), 118.86 (Ph- C_3 and C_5), 111.88 (pyrrole- C_3 and C_4), 105.22 (thiazole- C_5); MS (ESI): m/z = found 260.02 [M^+], 262.02 [$\text{M}^+ + 2$], 235, 217, 196/194, 150, 118; calcd. 260.74. Anal. $\text{C}_{13}\text{H}_9\text{ClN}_2\text{S}$.

4-(4-Hydroxyphenyl)-2-(1H-pyrrol-1-yl)thiazole (12c) Yield 70 %. mp 103–105 °C; FTIR (KBr): 3351 (OH), 2919 and 2852 (Ar-H), 1606 (C=N) cm^{-1} ; ^1H NMR (400 MHz, CDCl_3) δ ppm: 6.37 (dd, 2H, pyrrole- C_3 and C_4 -H), 6.89–6.92 (m, 2H, Ph- C_3 and C_5 -H), 6.99 (s, 1H, thiazole- C_5 -H), 7.42 (dd, 2H, pyrrole- C_2 and C_5 -H), 7.78–7.82 (m, 2H, Ph- C_2 and C_6 -H), 8.50 (s, 1H, OH); ^{13}C NMR (400 MHz, CDCl_3) δ ppm: 159.61 (thiazole- C_2), 157.49 (Ph- C_4), 151.86 (thiazole- C_4), 127.11 (Ph- C_2 and C_6), 124.97 (Ph- C_1), 119.11 (pyrrole- C_2 and C_5), 115.27 (Ph- C_3 and C_5), 111.57 (pyrrole- C_3 and C_4), 104.74 (thiazole- C_5); MS (ESI): m/z = found 242.05 [M^+], 192, 177, 176, 161; calcd. 242.30. Anal. $\text{C}_{13}\text{H}_{10}\text{N}_2\text{O}_2\text{S}$.

4-(4-Bromophenyl)-2-(1H-pyrrol-1-yl)thiazole (12d) Yield 63 %. mp 115–117 °C; FTIR (KBr): 2922 and 2855 (Ar-H), 1641 (C=N) cm^{-1} ; ^1H NMR (400 MHz, CDCl_3) δ ppm: 6.28 (dd, 2H, pyrrole- C_3 and C_4 -H), 7.04 (s, 1H, thiazole- C_5 -H), 7.31 (dd, 2H, pyrrole- C_2 and C_5 -H), 7.45–7.48 (m, 2H, Ph- C_3 and C_5 -H), 7.67–7.70 (m, 2H, Ph- C_2 and C_6 -H); ^{13}C NMR (400 MHz, CDCl_3) δ ppm: 160.73 (thiazole- C_2), 151.43 (thiazole- C_4), 132.96 (Ph- C_1), 131.86 (Ph- C_3 and C_5), 127.78 (Ph- C_2 and C_6), 122.34 (Ph- C_4), 119.69 (pyrrole- C_2 and C_5), 112.15 (pyrrole- C_3 and C_4), 107.29 (thiazole- C_5); MS (ESI): m/z = found 305.96 [M^+], 303.97 [$\text{M}^+ - 2$], 291, 293, 238/240, 175; calcd. 305.19. Anal. $\text{C}_{13}\text{H}_9\text{BrN}_2\text{S}$.

4-(4-Methoxyphenyl)-2-(1H-pyrrol-1-yl)thiazole (12e) Yield 77 %. mp 105–107 °C; FTIR (KBr): 2918 and 2848 (Ar-H), 1609 (C=N) cm^{-1} ; ^1H NMR (500 MHz, CDCl_3) δ ppm: 3.81 (s, 3H, OCH_3), 6.39 (dd, 2H, pyrrole- C_3 and C_4 -H), 7.16 (s, 1H, thiazole- C_5 -H), 7.28–7.95 (m, 6H, Ph- C_2 , C_3 , C_5 and C_6 -H, pyrrole- C_2 and C_5 -H); ^{13}C NMR (400 MHz, CDCl_3) δ ppm: 160.45 (Ph- C_4), 159.76 (thiazole- C_2), 152.41 (thiazole- C_4), 127.55 (Ph- C_2 and C_6), 127.07 (Ph- C_1), 119.68 (pyrrole- C_2 and C_5), 114.09 (Ph- C_3 and C_5), 111.87 (pyrrole- C_3 and C_4), 105.03 (thiazole- C_5), 55.36 (OCH_3); MS (ESI): m/z = found 256.07 [M^+], 191, 150, 161, 119, 85, 78; calcd. 256.32. Anal. $\text{C}_{14}\text{H}_{12}\text{N}_2\text{O}_2\text{S}$.

4-(4-Nitrophenyl)-2-(1H-pyrrol-1-yl)thiazole (12f) Yield 68 %. mp 68–70 °C; FTIR (KBr): 2918 and 2851 (Ar-H), 1608 (C=N), 1502, and 1337 (NO_2) cm^{-1} ; ^1H NMR (500 MHz, CDCl_3) δ ppm: 6.32 (dd, 2H, pyrrole- C_3 and C_4 -H), 7.10 (s, 1H, thiazole- C_5 -H), 7.35–8.12 (m, 6H, Ph- C_2 , C_3 , C_5 and C_6 -H, pyrrole- C_2 and C_5 -H); ^{13}C NMR (300 MHz, DMSO) δ = ^{13}C NMR (400 MHz, CDCl_3) δ ppm: 161.45 (Ph- C_4), 158.45 (thiazole- C_2), 151.88 (thiazole- C_4), 130.25 (Ph- C_3 and C_5), 129.66 (Ph- C_2 and C_6), 128.54 (Ph- C_1), 119.20 (pyrrole- C_2 and C_5), 111.52 (pyrrole- C_3 and C_4), 108.12 (thiazole- C_5); MS (ESI): m/z = found 271.04 [M^+], 150, 119, 85; calcd. 271.29. Anal. $\text{C}_{13}\text{H}_9\text{N}_3\text{O}_2\text{S}$.

4-(4-Aminophenyl)-2-(1H-pyrrol-1-yl)thiazole (12g) Yield 89 %. mp 127–129 °C; FTIR (KBr): 3220 (NH_2), 2920, 2852 (Ar-H), 1609 (C=N) cm^{-1} ; ^1H NMR (400 MHz, CDCl_3) δ ppm: 5.34 (s, 2H, NH_2), 6.28 (dd, 2H, pyrrole- C_3 and C_4 -H), 7.31 (dd, 2H, pyrrole- C_2 and C_5 -H), 7.35–7.51 (m, 4H, Ph- C_2 , C_3 , C_5 and C_6 -H), 8.06 (s, 1H, thiazole- C_5 -H); ^{13}C NMR (400 MHz, CDCl_3) δ ppm: 159.74 (thiazole- C_2), 158.22 (Ph- C_4), 150.56 (thiazole- C_4), 129.32 (Ph- C_2 and C_6), 125.78 (Ph- C_1), 120.90 (pyrrole- C_2 and C_5), 116.58 (Ph- C_3 and C_5), 111.23 (pyrrole- C_3 and C_4), 105.22 (thiazole- C_5); MS (ESI): m/z = found 241.07 [M^+], 150, 119, 85; calcd. 241.31. Anal. $\text{C}_{13}\text{H}_{11}\text{N}_3\text{S}$.

4-(4-Fluorophenyl)-2-(1H-pyrrol-1-yl)thiazole (12h) Yield 60 %. mp 106–108 °C; FTIR (KBr): 2989, 2941 (Ar-H), 1599 (C=N) cm^{-1} ; ^1H NMR (400 MHz, CDCl_3) δ ppm: 6.41 (dd, 2H, pyrrole- C_3 and C_4 -H), 7.13 (d, 2H, $J = 8$ Hz, Ph- C_3 and C_5 -H), 7.26 (dd, 2H, pyrrole- C_2 and C_5 -H), 7.31 (s, 1H, thiazole- C_5 -H), 7.79–7.91 (m, 2H, Ph- C_2 and C_6 -H); ^{13}C NMR (400 MHz, CDCl_3) δ ppm: 161.53 (Ph- C_4), 159.71 (thiazole- C_2), 152.13 (thiazole- C_4), 135.21 (Ph- C_2 and C_6), 130.57 (Ph- C_1), 129.13 (pyrrole- C_2 and C_5), 123.01 (Ph- C_3 and C_5), 110.41 (pyrrole- C_3 and C_4), 108.45 (thiazole- C_5); MS (ESI): m/z = found 244.05 [M^+], 150, 119, 95, 85; calcd. 244.29. Anal. $\text{C}_{13}\text{H}_9\text{FN}_2\text{S}$.

4-(3,4-Dichlorophenyl)-2-(1H-pyrrol-1-yl)thiazole (12i) Yield 77 %. mp 126–128 °C; FTIR (KBr): 2969, 2921 (Ar-H), 1593 (C=N) cm^{-1} ; ^1H NMR (400 MHz, CDCl_3) δ ppm: 6.39 (dd, 2H, pyrrole- C_3 and C_4 -H), 7.19 (s, 1H, thiazole- C_5 -H), 7.31 (dd, 2H, pyrrole- C_2 and C_5 -H), 7.53–7.91 (m, 3H, Ph- C_3 , C_4 and C_6 -H), 7.79–7.91 (m, 2H, Ph- C_2 and C_6 -H); ^{13}C NMR (400 MHz, CDCl_3) δ ppm: 159.03 (thiazole- C_2), 150.81 (thiazole- C_4), 135.29 (Ph- C_4), 133.23 (Ph- C_3), 132.13 (Ph- C_1), 131.11 (Ph- C_5), 128.73 (Ph- C_2), 127.27 (Ph- C_6), 113.29 (pyrrole- C_2 and C_5), 109.10 (pyrrole- C_3 and C_4), 108.43 (thiazole- C_5); MS (ESI): m/z = found 295.98 [M^+], 293.98 [$\text{M}^+ - 2$], 150, 144/146, 119, 67; calcd. 295.19. Anal. $\text{C}_{13}\text{H}_8\text{Cl}_2\text{N}_2\text{S}$.

2-(1H-pyrrol-1-yl)-4-(3,4,5-trimethoxyphenyl)thiazole (12j) Yield 62 %. mp 144–146 °C; FTIR (KBr): 2921, 2883 (Ar–H), 1601 (C=N) cm^{-1} ; ^1H NMR (400 MHz, CDCl_3) δ ppm: 3.86 (s, 9H, 3OCH₃), 6.37 (dd, 2H, pyrrole–C₃ and C₄–H), 6.89 (d, 2H, $J = 7.5$ Hz, Ph–C₂ and C₆–H), 7.21 (s, 1H, thiazole–C₅–H), 7.49 (dd, 2H, pyrrole–C₂ and C₅–H); ^{13}C NMR (400 MHz, CDCl_3) δ ppm: 160.01 (thiazole–C₂), 154.29 (Ph–C₃ and C₅), 151.39 (thiazole–C₄), 142.22 (Ph–C₄), 129.53 (Ph–C₁), 115.29 (pyrrole–C₂ and C₅), 110.09 (pyrrole–C₃ and C₄), 109.87 (thiazole–C₅) 102.29 (Ph–C₂ and C₆), 61.73 (4-OCH₃), 56.89 (3,5-(OCH₃)₂); MS (ESI): $m/z =$ found 316.09 [M^+], 271, 250, 167, 150, 67; calcd. 316.37. Anal. C₁₆H₁₆N₂O₃S.

4-(3,4-Dimethoxyphenyl)-2-(1H-pyrrol-1-yl)thiazole (12k) Yield 62 %. mp 132–134 °C; FTIR (KBr): 2923, 2849 (Ar–H), 1601 (C=N) cm^{-1} ; ^1H NMR (400 MHz, CDCl_3) δ ppm: 3.90 (s, 6H, 2OCH₃), 6.39 (dd, 2H, pyrrole–C₃ and C₄–H), 7.11 (s, 1H, thiazole–C₅–H), 7.21–8.03 (m, 5H, Ph–C₂, C₅ and C₆–H, pyrrole–C₂ and C₅–H); ^{13}C NMR (400 MHz, CDCl_3) δ ppm: 159.84 (thiazole–C₂), 151.27 (thiazole–C₄), 150.85 (Ph–C₃), 150.31 (Ph–C₄), 130.22 (Ph–C₁), 117.11 (pyrrole–C₂ and C₅), 115.27 (Ph–C₆), 113.03 (Ph–C₅), 110.27 (pyrrole–C₃, C₄ and Ph–C₂), 109.15 (thiazole–C₅), 56.81 (3,4-(OCH₃)₂); MS (ESI): $m/z =$ found 286.08 [M^+], 254, 220, 150, 137; calcd. 286.35. Anal. C₁₅H₁₄N₂O₂S.

4-(3-Nitrophenyl)-2-(1H-pyrrol-1-yl)thiazole (12l) Yield 59 %. mp 107–109 °C; FTIR (KBr): 2920, 2879 (Ar–H), 1607 (C=N), 1502, 1331 (NO₂) cm^{-1} ; ^1H NMR (400 MHz, CDCl_3) δ ppm: 6.35 (dd, 2H, pyrrole–C₃ and C₄–H), 7.03 (s, 1H, thiazole–C₅–H), 7.41–8.19 (m, 6H, Ph–C₂, C₄, C₅ and C₆–H, pyrrole C₂ and C₅–H); ^{13}C NMR (400 MHz, CDCl_3) δ ppm: 160.09 (thiazole–C₂), 150.33 (thiazole–C₄), 149.11 (Ph–C₃), 134.21 (Ph–C₁), 133.29 (Ph–C₆), 131.45 (Ph–C₂), 125.25 (Ph–C₄), 123.81 (Ph–C₅), 115.19 (pyrrole–C₂ and C₅), 109.10 (pyrrole–C₃ and C₄), 108.81 (thiazole–C₅); MS (ESI): $m/z =$ found 271.04 [M^+], 205, 150, 149, 124, 122; calcd. 271.29. Anal. C₁₃H₉N₃O₂S.

General procedure for the preparation of 4-(4-substituted phenyl)-2-(2,5-dimethyl-1H-pyrrol-1-yl)thiazoles (13a–l)

To a solution of 2-amino-4-(4-substituted phenyl)thiazoles (10 mmol) in 20 mL glacial acetic acid, acetyl acetone (15 mmol) was added slowly at room temperature and was refluxed for 1 h (monitored by TLC). The reaction mixture was poured into ice-cold water and basified with ammonium carbonate solution. The separated solid was collected, washed with water, and dried. The compounds were purified by column chromatography using chromatotron (hexane/ethyl acetate 70:30).

4-Phenyl-2-(2,5-dimethyl-1H-pyrrol-1-yl)thiazole (13a) Yield 67 %. mp 60–62 °C; FTIR (KBr): 2920 and 2853 (Ar–H), 1598 (C=N) cm^{-1} ; (400 MHz, CDCl_3) δ ppm: 2.18 (s, 6H, 2CH₃), 5.75 (s, 2H, pyrrole–C₃ and C₄–H), 7.28–7.36 (m, 3H, Ph–C₃, C₄ and C₅–H), 7.50 (s, 1H, thiazole–C₅–H), 7.88–8.10 (m, 2H, Ph–C₂ and C₆–H); MS (ESI): $m/z =$ found 254.09 [M^+], 210, 178, 160, 95, 85; calcd. 254.35. Anal. C₁₅H₁₄N₂S.

4-(4-Chlorophenyl)-2-(2,5-dimethyl-1H-pyrrol-1-yl)thiazole (13b) Yield 82 %. mp 58–60 °C; FTIR (KBr): 2956 and 2919 (Ar–H), 1654 (C=N) cm^{-1} ; ^1H NMR (400 MHz, CDCl_3) δ ppm: 2.21 (s, 6H, 2CH₃), 5.85 (s, 2H, pyrrole–C₃ and C₄–H), 7.31–7.34 (m, 2H, Ph–C₃ and C₅–H), 7.38 (s, 1H, thiazole–C₅–H), 7.76–7.79 (m, 2H, Ph–C₂ and C₆–H); ^{13}C NMR (400 MHz, CDCl_3) δ ppm: 158.87 (thiazole–C₂), 151.54 (thiazole–C₄), 134.23 (Ph–C₄), 132.59 (Ph–C₁), 129.89 (Ph–C₃ and C₅), 129.04 (Ph–C₂ and C₆), 127.50 (pyrrole–C₂ and C₅), 112.75 (pyrrole–C₃ and C₄), 108.26 (thiazole–C₅), 13.53 (2CH₃); MS (ESI): $m/z =$ found 288.05 [M^+], 290.05 [$\text{M}^+ + 2$], 210, 176, 95, 85; calcd. 288.80. Anal. C₁₅H₁₃ClN₂S.

4-(4-Hydroxyphenyl)-2-(2,5-dimethyl-1H-pyrrol-1-yl)thiazole (13c) Yield 75 %. mp 108–110 °C; FTIR (KBr): 3221 (OH), 2920 and 2854 (Ar–H), 1655 (C=N) cm^{-1} ; ^1H NMR (400 MHz, DMSO-*d*₆) δ ppm: 2.17 (s, 6H, 2CH₃), 5.79 (s, 2H, pyrrole–C₃ and C₄–H), 6.79 (d, 2H, $J = 11$ Hz, Ph–C₃ and C₅–H), 7.44 (s, 1H, thiazole–C₅–H), 7.67 (d, 2H, $J = 11$ Hz, Ph–C₂ and C₆–H), 9.25 (bs, 1H, OH); ^{13}C NMR (400 MHz, DMSO-*d*₆) δ ppm: 157.53 (thiazole–C₂ and Ph–C₄), 152.12 (thiazole–C₄), 128.92 (Ph–C₂ and C₆), 127.06 (pyrrole–C₂ and C₅), 125.02 (Ph–C₁), 115.34 (Ph–C₃ and C₅), 110.42 (pyrrole–C₃ and C₄), 107.57 (thiazole–C₅), 12.96 (2CH₃); MS (ESI): $m/z =$ found 270.08 [M^+], 192, 177, 176, 161, 95, 85; calcd. 270.35. Anal. C₁₅H₁₄N₂OS.

4-(4-Bromophenyl)-2-(2,5-dimethyl-1H-pyrrol-1-yl)thiazole (13d) Yield 87 %. mp 84–86 °C; FTIR (KBr): 2981 and 2952 (Ar–H), 1617 (C=N) cm^{-1} ; ^1H NMR (400 MHz, CDCl_3) δ ppm: 2.20 (s, 6H, 2CH₃), 5.84 (s, 2H, pyrrole–C₃ and C₄–H), 7.39 (s, 1H, thiazole–C₅–H), 7.46–7.48 (m, 2H, Ph–C₃ and C₅–H), 7.70–7.72 (m, 2H, Ph–C₂ and C₆–H); ^{13}C NMR (400 MHz, CDCl_3) δ ppm: 158.90 (thiazole–C₂), 151.57 (thiazole–C₄), 133.03 (Ph–C₃ and C₅), 132.01 (Ph–C₁), 129.89 (Ph–C₂ and C₆), 127.81 (pyrrole–C₂ and C₅), 122.48 (Ph–C₄), 112.87 (pyrrole–C₃ and C₄), 108.32 (thiazole–C₅), 13.59 (2CH₃); MS (ESI): $m/z =$ found 332.00 [M^+], 334.00 [$\text{M}^+ + 2$], 176, 160, 157, 95, 85; calcd. 332.00. Anal. C₁₅H₁₃BrN₂S.

Table 3 In vitro antibacterial activity of pyrrole derivatives (**5a–m**, **8a–m**, **12a–l**, and **13a–l**) against the selected strains (MIC in $\mu\text{g/mL}$)

Compound	Gram-positive bacteria		Gram-negative bacteria	
	<i>S. aureus</i>	<i>B. subtilis</i>	<i>K. pneumoniae</i>	<i>E. coli</i>
5a	12.5	0.8	3.125	1.6
5b	12.5	3.125	6.25	12.5
5c	6.25	0.8	1.6	0.8
5d	3.125	1.6	1.6	0.8
5e	3.125	0.4	1.6	1.6
5f	6.25	1.6	12.5	12.5
5g	6.25	0.4	3.125	12.5
5h	3.125	0.2	1.6	0.8
5i	6.25	0.8	12.5	12.5
5j	12.5	3.125	3.125	12.5
5k	6.25	1.6	3.125	1.6
5l	12.5	3.125	6.25	12.5
5m	12.5	3.125	6.25	12.5
8a	12.5	3.125	3.125	12.5
8b	12.5	3.125	6.25	12.5
8c	3.125	1.6	6.25	12.5
8d	6.25	1.6	6.25	1.6
8e	3.125	0.8	12.5	12.5
8f	3.125	0.4	1.6	0.8
8g	6.25	1.6	3.125	1.6
8h	3.125	0.2	1.6	1.6
8i	12.5	3.125	3.125	12.5
8j	12.5	3.125	12.5	6.25
8k	6.25	1.6	3.125	6.25
8l	6.25	1.6	6.25	12.5
8m	12.5	3.125	12.5	12.5
12a	0.8	0.4	25	25
12b	1.6	0.4	12.5	50
12c	12.5	25	12.5	25
12d	1.6	1.6	100	50
12e	12.5	3.12	100	50
12f	0.4	0.2	6.25	12.5
12g	12.5	25	12.5	25
12h	1.6	0.2	3.12	12.5
12i	1.6	1.6	12.5	25
12j	12.5	3.12	50	50
12k	12.5	6.25	50	50
12l	1.6	1.6	12.5	50
13a	1.6	0.8	12.5	12.5
13b	12.5	6.25	50	50
13c	0.8	12.5	100	100
13d	0.8	0.8	100	100
13e	1.6	1.6	50	50
13f	0.4	0.2	3.12	12.5
13g	0.4	1.6	50	50
13h	0.4	0.2	3.12	12.5

Table 3 continued

Compound	Gram-positive bacteria		Gram-negative bacteria	
	<i>S. aureus</i>	<i>B. subtilis</i>	<i>K. pneumoniae</i>	<i>E. coli</i>
13i	0.8	0.4	6.25	12.5
13j	25	25	50	50
13k	12.5	6.25	100	50
13l	1.6	1.6	100	100
Ciprofloxacin	2	2	1	2
Norfloxacin	3	1	1	12

4-(4-Methoxyphenyl)-2-(2,5-dimethyl-1H-pyrrol-1-yl)thiazole (13e) Yield 80 %. mp 61–63 °C; FTIR (KBr): 3092 and 2925 (Ar-H), 1609 (C=N) cm^{-1} ; ^1H NMR (500 MHz, CDCl_3) δ ppm: 2.30 (s, 6H, 2CH₃), 3.88 (s, 3H, OCH₃), 5.94 (s, 2H, pyrrole-C₃ and C₄-H), 6.99 (d, 2H, $J = 9$ Hz, Ph-C₃ and C₅-H), 7.36 (s, 1H, thiazole-C₅-H), 7.89 (d, 2H, $J = 9$ Hz, Ph-C₂ and C₆-H); ^{13}C NMR (400 MHz, CDCl_3) δ ppm: 159.82 (Ph-C₄), 158.46 (thiazole-C₂), 152.56 (thiazole-C₄), 129.90 (Ph-C₂ and C₆), 127.52 (pyrrole-C₂ and C₅), 127.04 (Ph-C₁), 114.18 (Ph-C₃ and C₅), 110.68 (pyrrole-C₃ and C₄), 107.91 (thiazole-C₅), 55.38 (OCH₃), 13.40 (2CH₃); MS (ESI): $m/z =$ found 284.10 [M^+], 242, 207, 95, 85; calcd. 284.38. Anal. C₁₆H₁₆N₂OS.

4-(4-Nitrophenyl)-2-(2,5-dimethyl-1H-pyrrol-1-yl)thiazole (13f) Yield 64 %. mp 65–67 °C; FTIR (KBr): 2921 and 2858 (Ar-H), 1646 (C=N), 1506, 1339 (NO₂) cm^{-1} ; ^1H NMR (400 MHz, CDCl_3) δ ppm: 2.31 (s, 6H, 2CH₃), 5.95 (s, 2H, pyrrole-C₃ and C₄-H), 7.69 (s, 1H, thiazole-C₅-H), 8.06–8.10 (m, 2H, Ph-C₃ and C₅-H), 8.28–8.32 (m, 2H, Ph-C₂ and C₆-H); ^{13}C NMR (300 MHz, DMSO) $\delta =$ ^{13}C NMR (400 MHz, CDCl_3) δ ppm: 160.13 (Ph-C₄), 158.03 (thiazole-C₂), 151.27 (thiazole-C₄), 130.11 (Ph-C₃ and C₅), 129.47 (Ph-C₂ and C₆), 128.01 (pyrrole-C₂ and C₅), 127.33 (Ph-C₁), 111.09 (pyrrole-C₃ and C₄), 107.93 (thiazole-C₅), 13.43 (2CH₃); MS (ESI): $m/z =$ found 299.07 [M^+], 95, 85; calcd. 299.35. Anal. C₁₅H₁₃N₃O₂S.

4-(4-Aminophenyl)-2-(2,5-dimethyl-1H-pyrrol-1-yl)thiazole (13g) Yield 88 %. mp 137–139 °C; FTIR (KBr): 3437 (NH₂), 2920 and 2852 (Ar-H), 1612 (C=N) cm^{-1} ; ^1H NMR (400 MHz, CDCl_3) δ ppm: 2.22 (s, 6H, 2CH₃), 5.84 (s, 2H, NH₂), 5.85 (s, 2H, pyrrole-C₃ and C₄-H), 7.17 (s, 1H, thiazole-C₅-H), 7.19–7.21 (m, 2H, Ph-C₃ and C₅-H), 7.93–7.95 (m, 2H, Ph-C₂ and C₆-H); ^{13}C NMR (400 MHz, CDCl_3) δ ppm: 158.92 (thiazole-C₂), 151.84 (thiazole-C₄), 138.96 (Ph-C₄), 129.91 (Ph-C₂ and C₆), 128.63 (pyrrole-C₂ and C₅), 126.85 (Ph-C₁), 112.96 (Ph-C₃ and C₅), 108.14 (pyrrole-C₃ and C₄), 105.94 (thiazole-C₅), 13.47

Table 4 Antimycobacterial and cytotoxicity activity of pyrrole derivatives (**5a–m**, **8a–m**, **12a–l**, and **13a–l**)

Compound	<i>M. tuberculosis</i> H ₃₇ Rv ^a	IC ₅₀ (μM) ^b	
		MV cell lines ^c	A ₅₄₉ ^d
5a	6.25	NT	NT
5b	6.25	NT	NT
5c	0.8	NT	NT
5d	3.125	NT	NT
5e	0.4	251.22 ± 0.3	254.31 ± 0.3
5f	0.8	NT	NT
5g	0.4	259.19 ± 0.2	255.11 ± 0.3
5h	0.2	265.40 ± 0.3	261.12 ± 0.4
5i	0.8	NT	NT
5j	3.125	NT	NT
5k	3.125	NT	NT
5l	3.125	NT	NT
5m	3.125	NT	NT
8a	12.5	NT	NT
8b	12.5	NT	NT
8c	3.125	NT	NT
8d	3.125	NT	NT
8e	0.4	251.52 ± 0.3	234.82 ± 0.4
8f	0.4	251.34 ± 0.6	251.12 ± 0.3
8g	0.4	252.29 ± 0.5	250 ± 0.4
8h	0.2	260.13 ± 0.2	260.33 ± 0.3
8i	0.8	NT	NT
8j	6.25	NT	NT
8k	6.25	NT	NT
8l	6.25	NT	NT
8m	6.25	NT	NT
12a	0.4	233.21 ± 0.4	231.22 ± 0.4
12b	0.4	242.42 ± 0.5	244.61 ± 0.3
12c	50	NT	NT
12d	0.8	NT	NT
12e	12.5	NT	NT
12f	0.4	243.17 ± 0.6	246.09 ± 0.7
12g	25	NT	NT
12h	0.2	261.31 ± 0.3	262.57 ± 0.3
12i	0.8	NT	NT
12j	50	NT	NT
12k	50	NT	NT
12l	0.8	NT	NT
13a	0.4	NT	NT
13b	0.8	NT	NT
13c	12.5	NT	NT
13d	0.4	257.07 ± 0.6	253.29 ± 0.5
13e	6.25	NT	NT
13f	0.4	252.81 ± 0.7	253.13 ± 0.9
13g	12.5	NT	NT
13h	0.2	265.53 ± 0.3	268.34 ± 0.5

Table 4 continued

Compound	<i>M. tuberculosis</i> H ₃₇ Rv ^a	IC ₅₀ (μM) ^b	
		MV cell lines ^c	A ₅₄₉ ^d
13i	0.4	221.34 ± 0.5	231.67 ± 0.5
13j	12.5	NT	NT
13k	50	NT	NT
13l	0.8	NT	NT
Isoniazid	0.25	>450	>450
Cisplatin	–	1.29	9.90

NT not tested, ^cMV mammalian Vero cell lines, ^dA₅₄₉ lung adenocarcinoma cell lines

^a Minimal inhibition concentration is expressed in μg/mL

^b Cytotoxicity is expressed as IC₅₀, is the concentration of compound, which is reduced by 50 % of the optical density of treated cells with respect to untreated cells using the MTT assay, values are mean ± SEM of three independent experiments

(2CH₃); MS (ESI): *m/z* = found 269.10 [M⁺], 239, 175, 118, 95, 85; calcd. 269.36. Anal. C₁₅H₁₅N₃S.

4-(4-Fluorophenyl)-2-(1H-pyrrol-1-yl)thiazole (13h) Yield 57 %. mp 116–118 °C; FTIR (KBr): 2986 and 2920 (Ar–H), 1631 (C=N) cm⁻¹; ¹H NMR (400 MHz, CDCl₃) δ ppm: 2.29 (s, 6H, 2CH₃), 5.83 (s, 2H, pyrrole–C₃ and C₄–H), 7.29 (d, 2H, *J* = 8 Hz, Ph–C₃ and C₅–H), 7.41 (s, 1H, thiazole–C₅–H), 7.63 (d, 2H, *J* = 8 Hz, Ph–C₂ and C₆–H); ¹³C NMR (400 MHz, CDCl₃) δ ppm: 163.01 (Ph–C₄), 161.11 (thiazole–C₂), 151.29 (thiazole–C₄), 133.20 (Ph–C₂ and C₆), 129.01 (pyrrole–C₂ and C₅), 128.63 (Ph–C₁), 117.27 (Ph–C₃ and C₅), 111.08 (pyrrole–C₃ and C₄), 108.21 (thiazole–C₃), 12.76 (2CH₃); MS (ESI): *m/z* = found 272.08 [M⁺], 178, 146, 95; calcd. 272.34. Anal. C₁₅H₁₃FN₂S.

4-(3,4-Dichlorophenyl)-2-(1H-pyrrol-1-yl)thiazole (13i) Yield 75 %. mp 140–142 °C; FTIR (KBr): 2990 and 2957 (Ar–H), 1627 (C=N) cm⁻¹; ¹H NMR (400 MHz, CDCl₃) δ ppm: 2.20 (s, 6H, 2CH₃), 5.87 (s, 2H, pyrrole–C₃ and C₄–H), 7.31–7.69 (m, 4H, thiazole–C₅–H, Ph–C₃, C₅, C₆–H); ¹³C NMR (400 MHz, CDCl₃) δ ppm: 159.81 (thiazole–C₂), 150.78 (thiazole–C₄), 135.43 (Ph–C₄), 133.09 (Ph–C₃), 132.83 (Ph–C₁), 131.52 (Ph–C₅), 129.88 (Ph–C₂), 128.01 (Ph–C₆), 127.89 (pyrrole–C₂ and C₅), 110.22 (pyrrole–C₃ and C₄), 109.02 (thiazole–C₅), 12.82 (2CH₃); MS (ESI): *m/z* = found 322.01 [M⁺], 324.01 [M⁺+2], 232/230, 178, 144/146, 95; calcd. 323.24. Anal. C₁₅H₁₂Cl₂N₂S.

2-(1H-pyrrol-1-yl)-4-(3,4,5-trimethoxyphenyl)thiazole (13j) Yield 65 %. mp 159–161 °C; FTIR (KBr): 2977 and 2913 (Ar–H), 1605 (C=N) cm⁻¹; ¹H NMR (400 MHz, CDCl₃) δ ppm: 2.27 (s, 6H, 2CH₃), 3.89 (s, 9H, (OCH₃)₃), 5.97 (s, 2H, pyrrole–C₃ and C₄–H), 7.97 (s, 1H, thiazole–C₅–H),

7.63 (d, 2H, $J = 7.5$ Hz, Ph-C₂ and C₆-H); ¹³C NMR (400 MHz, CDCl₃) δ ppm: 159.37 (thiazole-C₂), 154.07 (Ph-C₃ and C₅), 150.21 (thiazole-C₄), 140.81 (Ph-C₄), 128.09 (Ph-C₁), 127.31 (pyrrole-C₂ and C₅), 110.21 (pyrrole-C₃ and C₄), 109.59 (thiazole-C₅), 103.19 (Ph-C₂ and C₆), 60.53 (4-OCH₃), 57.22 (3,5-(OCH₃)₂), 12.90 (2CH₃); MS (ESI): $m/z =$ found 344.12 [M⁺], 312, 178, 167, 95; calcd. 344.43. Anal. C₁₈H₂₀N₂O₃S.

4-(3,4-Dimethoxyphenyl)-2-(1H-pyrrol-1-yl)thiazole (13k) Yield 67 %. mp 146–148 °C; FTIR (KBr): 2939 and 2887 (Ar-H), 1621 (C=N) cm⁻¹; ¹H NMR (400 MHz, CDCl₃) δ ppm: 2.21 (s, 6H, 2CH₃), 3.83 (s, 6H, (OCH₃)₂), 5.84 (s, 2H, pyrrole-C₃ and C₄-H), 7.39–7.83 (m, 4H, thiazole-C₅-H, Ph-C₂, C₅ and C₆-H); ¹³C NMR (400 MHz, CDCl₃) δ ppm: 159.51 (thiazole-C₂), 150.87 (thiazole-C₄), 150.09 (Ph-C₃), 149.29 (Ph-C₄), 130.12 (Ph-C₁), 128.17 (pyrrole-C₂ and C₅), 123.01 (Ph-C₆), 120.19 (Ph-C₅), 117.81 (Ph-C₂), 111.19 (pyrrole-C₃, C₄), 109.27 (thiazole-C₅), 57.11 (3,4-(OCH₃)₂), 12.80 (2CH₃); MS (ESI): $m/z =$ found 314.11 [M⁺], 220, 178, 152, 137; calcd. 314.40. Anal. C₁₇H₁₈N₂O₂S.

4-(3-Nitrophenyl)-2-(1H-pyrrol-1-yl)thiazole (13l) Yield 50 %. mp 150–152 °C; FTIR (KBr): 2981 and 2909 (Ar-H), 1609 (C=N), 1507, 1333 (NO₂) cm⁻¹; ¹H NMR (400 MHz, CDCl₃) δ ppm: 2.30 (s, 6H, 2CH₃), 5.87 (s, 2H, pyrrole-C₃ and C₄-H), 7.61–8.21 (m, 5H, thiazole-C₅-H, Ph-C₂, C₄, C₅ and C₆-H); ¹³C NMR (400 MHz, CDCl₃) δ ppm: 159.23 (thiazole-C₂), 150.31 (thiazole-C₄), 149.01 (Ph-C₃), 134.03 (Ph-C₁), 133.27 (Ph-C₆), 131.13 (Ph-C₂), 127.59 (pyrrole-C₂ and C₅), 125.49 (Ph-C₄), 124.51 (Ph-C₅), 110.01 (pyrrole-C₃ and C₄), 109.03 (thiazole-C₅), 12.77 (2CH₃); MS (ESI): $m/z =$ found 299.07 [M⁺], 205, 178, 152, 145, 122, 95; calcd. 299.35. Anal. C₁₅H₁₃N₃O₂S.

Biological activities

In vitro antibacterial activity

MIC determination of the test compounds (**5a–m**, **8a–m**, **12a–l**, and **13a–l**) was investigated in side-by-side comparison with ciprofloxacin and norfloxacin against Gram-positive (*Staphylococcus aureus* and *Bacillus subtilis*) and Gram-negative bacteria (*Klebsiella pneumoniae* and

Escherichia coli) by broth microdilution method (Goto *et al.*, 1981). Serial dilutions of the test compounds and reference drugs were prepared in Mueller–Hinton agar. Drugs (10 mg) were dissolved in DMSO (1 mL). Further progressive dilutions with melted Mueller–Hinton agar were performed to obtain the required concentrations of 0.2, 0.4, 0.8, 1.6, 3.125, 6.25, 12.5, 25, 50, and 100 $\mu\text{g mL}^{-1}$. The tubes were inoculated with 10⁵ CFU mL⁻¹ (colony forming unit/mL) and incubated at 37 °C for 18 h. The MIC was the lowest concentration of the tested compound that yield no visible growth on the plate. To ensure that solvent had no effect on the bacterial growth, a control was performed with the test medium supplemented with DMSO at the same dilutions as used in the experiments and DMSO had no effect on the microorganisms in the concentrations studied. Table 3 reveals the antibacterial activity (MIC values) of the compounds.

MIC values were determined for the newly synthesized compounds (**5a–m**, **8a–m**, **12a–l**, and **13a–l**) against MTB strain H₃₇Rv using the microplate alamar blue assay (Franzblau *et al.*, 1998). Isoniazid was used as the standard drug. The 96-wells plate received 100 μL of the Middlebrook 7H9 broth and serial dilution of compounds were made directly on plate. The final drug concentrations tested were 0.2, 0.4, 0.8, 1.6, 3.125, 6.25, 12.5, 25, 50, and 100 $\mu\text{g mL}^{-1}$. Plates were covered and sealed with parafilm and incubated at 37 °C for 5 days. After this, 25 μL of freshly prepared 1:1 mixture of alamar blue reagent and 10 % Tween 80 was added to the plate and incubated for 24 h. A blue color in the well was interpreted as no bacterial growth and pink color was scored as growth. The MIC was defined as the lowest drug concentration which prevented the color change from blue to pink. Table 4 reveals the antitubercular activity (MIC) of the newly synthesized compounds.

MTT-based cytotoxic activity

The cellular conversion of MTT [3-(4,5-dimethylthiazol-2-yl)-2,5-diphenyl-tetrazolium bromide] into a formazan product (Mosmann, 1983) was used to evaluate the cytotoxic activity (IC₅₀) of some synthesized compounds against mammalian Vero cell lines and A₅₄₉ (lung adenocarcinoma) cell lines up to concentrations of 62.5 $\mu\text{g/mL}$ using the Promega Cell Titer 96 non-radioactive cell

Table 5 Statistical results of Topomer CoMFA including various parameters

q^2	StdErr	r^2	SEE	F value	Intercept	r^2_{pred}	PLS components
0.815	0.36	0.973	0.14	86.757	5.09	0.689	6

q^2 LOO cross-validation correlation coefficient, r^2 non-cross-validation correlation coefficient, *StdErr* standard error of prediction, *SEE* standard error of estimate, F Fischer test value, *Intercept* Y -intercept for the CoMFA model, r^2_{pred} predictive correlation coefficient, *PLS components* optimum number of components

Table 6 Actual and predicted antitubercular activity of the training set and the test set molecules with R₁ and R₂ fragments contributions

Compound	Fragments	Actual pMIC	Predicted pMIC	Fragment contributions	
				R ₁	R ₂
Training set					
5a	A1	5.20	5.12	0.30	-0.27
5b	A1	5.20	5.23	0.41	-0.27
5c	A1	6.10	5.87	1.05	-0.27
5d	A1	5.51	5.56	0.74	-0.27
5e	A1	6.40	6.47	1.65	-0.27
5f	A1	6.10	6.34	1.52	-0.27
5h(template)	T1	6.70	6.74	1.92	-0.27
5i	A1	6.10	6.15	1.33	-0.27
5j	A1	5.51	5.43	0.61	-0.27
5l	A1	5.51	5.49	0.67	-0.27
5m	A1	5.51	5.42	0.60	-0.27
8a	A1	4.90	4.99	0.30	-0.40
8c	A1	5.51	5.74	1.05	-0.40
8d	A1	5.51	5.43	0.74	-0.40
8e	A1	6.40	6.34	1.65	-0.40
8f	A1	6.40	6.21	1.52	-0.40
8g	A1	6.40	6.37	1.68	-0.40
8h	A1	6.70	6.61	1.92	-0.40
8i	A1	6.10	6.02	1.33	-0.40
8j	A1	5.20	5.30	0.61	-0.40
8k	A1	5.20	5.20	0.52	-0.40
8m	A1	5.20	5.29	0.60	-0.40
12a	A2	6.40	6.31	1.08	0.14
12b	A2	6.40	6.17	0.94	0.14
12c	A2	4.30	4.52	-0.71	0.14
12d	A2	6.10	6.20	0.97	0.14
12e	A2	4.90	5.01	-0.22	0.14
12f	A2	6.40	6.33	1.11	0.14
12h	A2	6.70	6.67	1.44	0.14
12i	A2	6.40	6.35	1.12	0.14
12j	A2	4.30	4.32	-0.91	0.14
12l	A2	6.10	6.12	0.89	0.14
13a	A2	6.40	6.42	1.08	0.26
13b	A2	6.10	6.29	0.94	0.26
13c	A2	4.90	4.63	-0.71	0.26
13d	A2	6.40	6.31	0.97	0.26
13e	A2	5.20	5.12	-0.22	0.26
13f	A2	6.40	6.45	1.11	0.26
13g	A2	4.90	4.97	-0.37	0.26
13h(template)	T2	6.70	6.78	1.44	0.26
13i	A2	6.40	6.46	1.12	0.26
13k	A2	4.30	4.26	-1.08	0.26
Test set					
5g	A1	6.40	6.50	1.68	-0.27

Table 6 continued

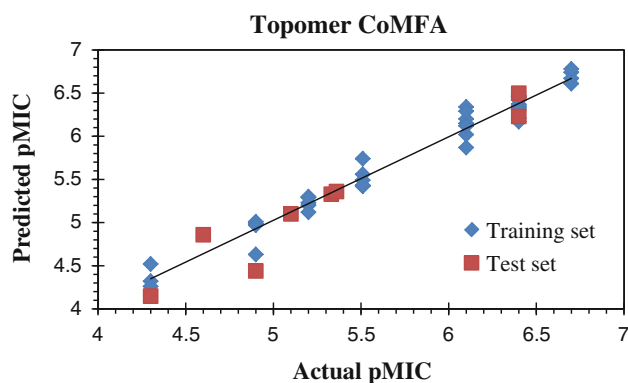
Compound	Fragments	Actual pMIC	Predicted pMIC	Fragment contributions	
				R ₁	R ₂
5k	A1	5.33	5.33	0.52	-0.27
8b	A1	5.10	5.10	0.41	-0.40
8l	A1	5.36	5.36	0.67	-0.40
12g	A2	4.60	4.86	-0.37	0.14
12k	A2	4.30	4.15	-1.08	0.14
13j	A2	4.90	4.44	-0.91	0.26
13l	A2	6.40	6.23	0.89	0.26

proliferation assay was employed (Gundersen *et al.*, 2002). Cisplatin was used as a positive control. The IC₅₀ values are the averages ± SEM of three independent experiments and are presented in Table 4.

Results and discussion

Synthetic and spectral studies

Structures of the compounds were assigned on the basis of their spectral and analytical data. The physical data, FTIR,

**Fig. 3** Scatter plot diagram for Topomer CoMFA analysis**Table 7** Topomer CoMFA contour map for the R₁ and R₂ fragments

Contours	R ₁			R ₂		
	Contour level	Color	Volume estimate	Contour level	Color	Volume estimate
Steric	-0.072	Yellow	3.5	-0.005	Yellow	4.1
	0.030	Green	72.0	0.003	Green	22.4
Electrostatic	-0.042	Red	14.8	-0.003	Red	23.2
	0.041	Blue	72.4	0.003	Blue	7.2

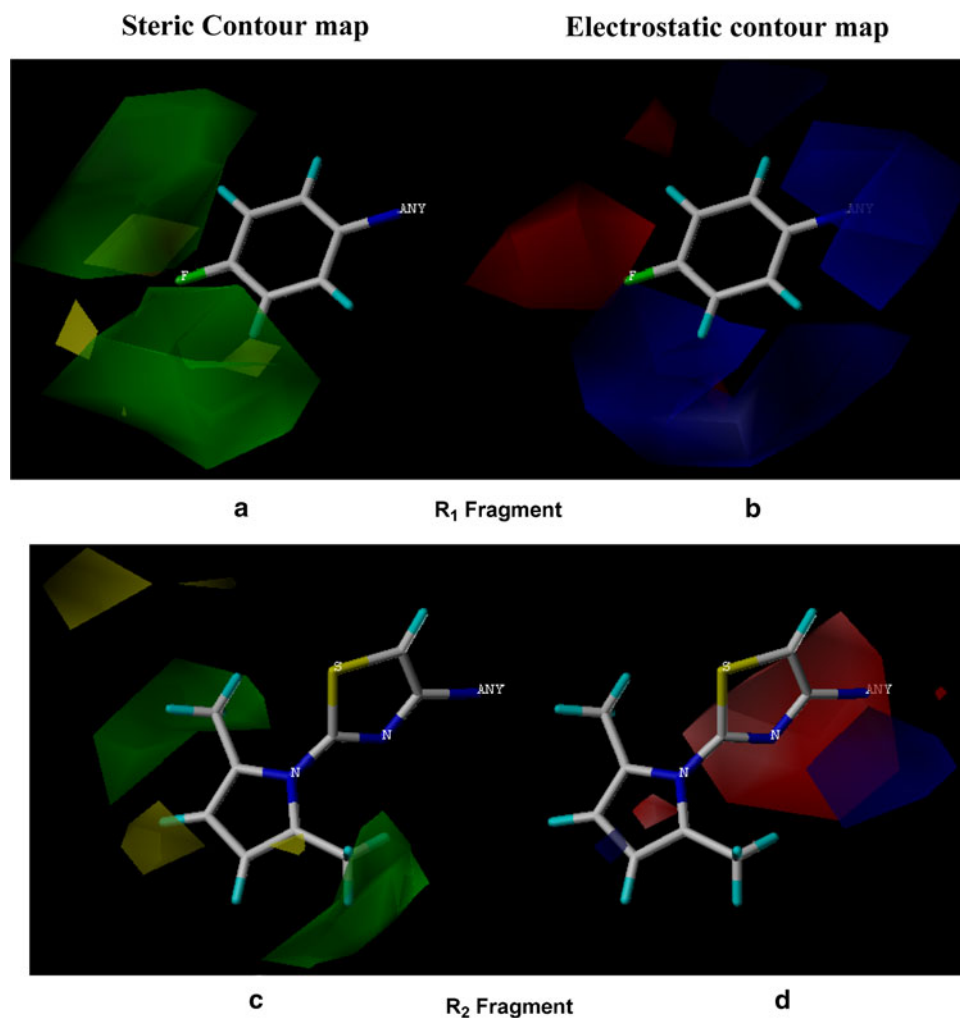
NMR, and MS are reported in the experimental protocols. The disappearance of NH₂ stretching band in the FTIR spectrum of **5e** confirmed the formation of pyrrolylimide. A strong stretching band at 1,728 cm⁻¹ was related to ketonic carbonyl. The ¹H NMR spectrum of **5e** showed a D₂O exchangeable singlet at δ 11.20 due to NH proton. The four protons of pyrrole ring appeared as two doublet of doublets at δ 6.35 and 7.32. The four protons of phenyl moiety resonated as two doublets at δ 7.64 and 8.13; the multiplets between δ 7.89 and 7.97 were assigned for four protons—C₄, C₅, C₆, and C₇ protons of isoindoline. Formation of pyrrolylimides was further confirmed by ¹³C NMR and MS. The ¹³C NMR spectrum of **5e** showed signals at δ 167.18, 165.38, and 164.52 due to isoindoline–C₅, isoindoline–C₂, and amide carbonyl carbons, respectively. MS showed accurate molecular ion peaks at *m/z* 281.08, 283.10, 296.10, 295.10, 331.10, 646.73, 468.94, 403.06, 400.02, 345.11, 376.08, 376.08, 337.14, 309.11, 311.13, 323.13, 323.13, 359.13, 674.76, 496.97, 431.09, 428.05, 373.14, 404.11, 404.11, and 365.17 for compounds **5a–m** and **8a–m**, respectively.

In the FTIR spectrum of **12c**, a broad absorption band observed at 3,351 cm⁻¹ was due to OH, while a strong stretching band at 1,606 cm⁻¹ was assigned to C=N. The ¹H NMR spectrum of **12c** showed a singlet at δ 8.50, which was accounted for hydroxyl group on the phenyl ring. A singlet at δ 6.99 was assigned to C₅ proton of thiazole; four protons of pyrrole moiety resonated as two doublet of doublets at δ 7.42 and 6.37. Multiplets between δ 6.89–6.92 and 7.78–7.82 were due to four aromatic protons. The MS of **12c** showed a molecular ion peak at *m/z* 242, which confirmed its molecular weight. Electron impact MS showed accurate molecular ion peaks at *m/z* 226.06, 260.02, 242.05, 305.96, 256.07, 271.04, 241.07, 244.05, 295.98, 316.09, 286.08, 271.04, 254.09, 288.05, 270.08, 332.00, 284.10, 299.07, 269.10, 272.08, 322.01, 344.12, 314.11, and 299.07 for compounds **12a–l** and **13a–l**, respectively.

Antimicrobial activity

The results of antimicrobial activities (expressed in MIC) of the compounds against the selected two Gram-positive,

Fig. 4 Steric and electrostatics stdev* coefficient contour map for compound **13h** by Topomer CoMFA analysis. **a** Steric contour map for the R₁ fragment. **b** Electrostatic contour map for the R₁ fragment. **c** Steric contour map for the R₂ fragment. **d** Electrostatics contour map for the R₂ fragment. Sterically favored/unfavored areas are shown in green/yellow contour, while the blue/red polyhedra depict the favorable sites for the positively/negatively charged groups (Color figure online)



two Gram-negative bacteria and MTB H₃₇Rv are illustrated in Tables 3 and 4, respectively. The activity of ciprofloxacin and norfloxacin are used for comparison. All the compounds showed moderate to significant microbial inhibition. Pyrrolylimide compounds showed antibacterial activity between MIC of 0.2 and 12.5 µg/mL. Compounds have shown better activity against *B. subtilis* than the other tested microorganisms. In pyrrolylimide series, compounds **5h** and **8h** showed the highest activity against *B. subtilis* at MIC of 0.2 µg/mL. Compounds **5c**, **d**, **h**, and **8f** showed the highest activity against *E. coli* at MIC of 0.8 µg/mL. Pyrrolythiazole compounds have exhibited antibacterial activity at MIC between 0.2 and 100 µg/mL and the compounds were more active against Gram-positive bacteria than Gram-negative bacteria. Compounds **12f**, **h**, **13f**,

and **h** have shown the highest activity against *B. subtilis* at MIC of 0.2 µg/mL (Table 3).

Antitubercular activity

The tested compounds (Schemes 1, 2) showed activities against mycobacteria with the MIC values ranging from 0.2 to 50 µg/mL (Table 4). The pyrrolylimide compounds showed antitubercular activity between MIC of 0.2 and 12.5 µg/mL. Among the pyrrolylimide derivatives, compounds **5h** and **8h** exhibited the highest activity against the tested mycobacteria at a MIC of 0.2 µg/mL. Similarly, pyrrolythiazole compounds **12h** and **13h** have shown the highest activity at MIC of 0.2 µg/mL against the tested mycobacteria.

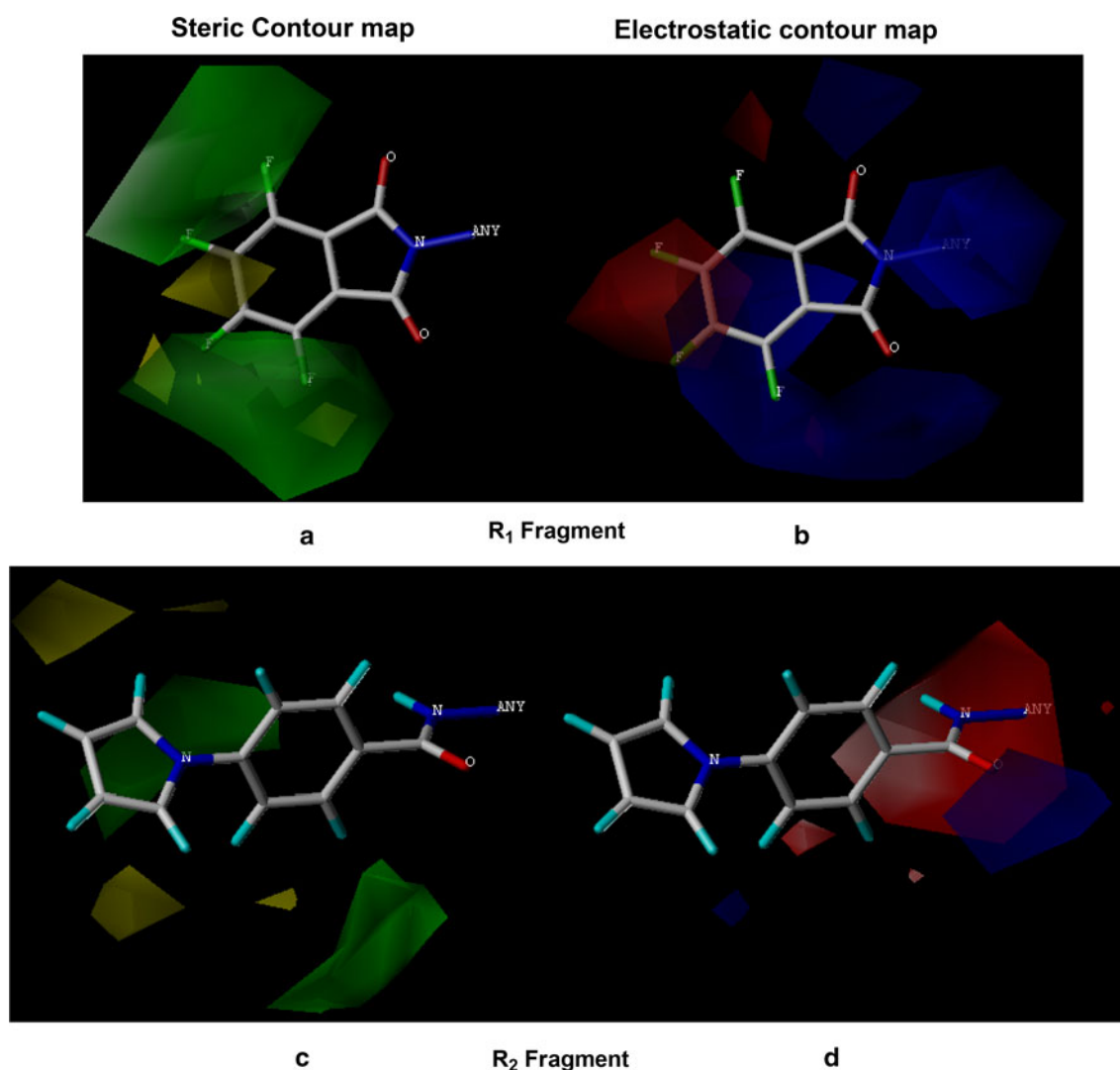


Fig. 5 Steric and electrostatics stdev* coefficient contour map for compound **5h** by Topomer CoMFA analysis. **a** Steric contour map for the R₁ fragment. **b** Electrostatic contour map for the R₁ fragment. **c** Steric contour map for the R₂ fragment. **d** Electrostatics contour map

for the R₂ fragment. Sterically favored/unfavored areas are shown in *green/yellow contour*, while the *blue/red polyhedra* depict the favorable sites for the positively/negatively charged groups (Color figure online)

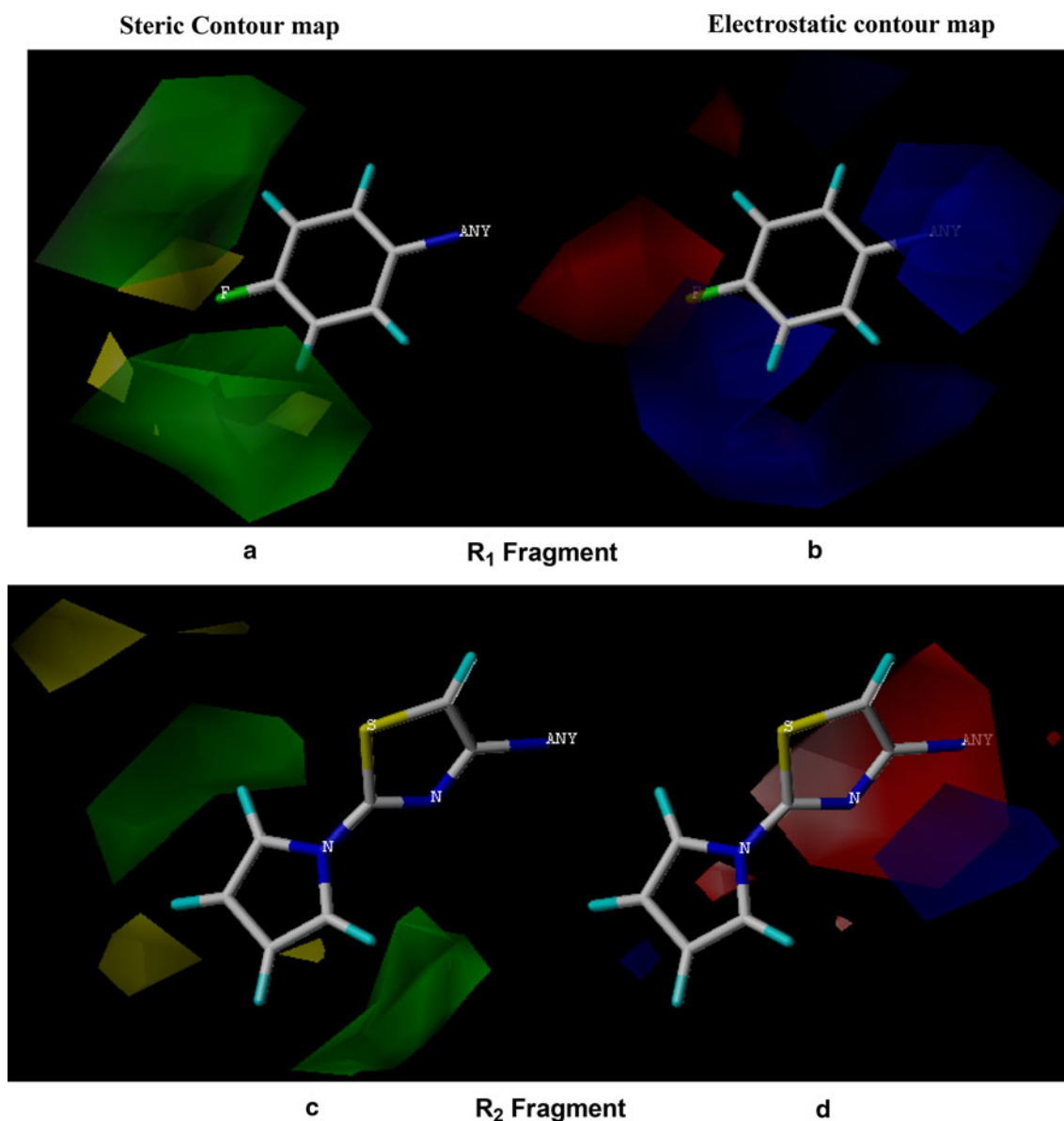


Fig. 6 Steric and electrostatics stdev* coefficient contour map for compound **12h** by Topomer CoMFA analysis. **a** Steric contour map for the R₁ fragment. **b** Electrostatic contour map for the R₁ fragment. **c** Steric contour map for the R₂ fragment. **d** Electrostatics contour

map for the R₂ fragment. Sterically favored/unfavored areas are shown in *green/yellow contour*, while the *blue/red polyhedra* depict the favorable sites for the positively/negatively charged groups (Color figure online)

Cytotoxic activity

Some compounds were further examined for toxicity (IC₅₀) in mammalian Vero cell lines and A₅₄₉ (lung adenocarcinoma) cell lines up to 62.5 μg/mL concentrations. After 72 h of exposure, viability was assessed on the basis of cellular conversion of MTT into a formazan product using the Promega Cell Titer 96 non-radioactive cell proliferation assay and the results are summarized in Table 4. The 15 derivatives tested showed IC₅₀ values ranging from 221.34 to 265.53 μM against mammalian Vero cell lines. However, all the compounds did not show any significant

activity against mammalian Vero cell line at concentrations <100 μM. Among the test compounds, pyrrolylimide derivatives showed inferior toxicity with IC₅₀ values of >250 μM against both mammalian Vero cell lines and A₅₄₉ (lung adenocarcinoma) cell lines.

QSAR study

Topomer CoMFA model analysis The model displayed a $q^2 = 0.815$ and $r^2 = 0.973$ with 0.36 StdErr and 0.14 standard error of estimate (SEE). The number of components that provided the highest q^2 was six. The summary of

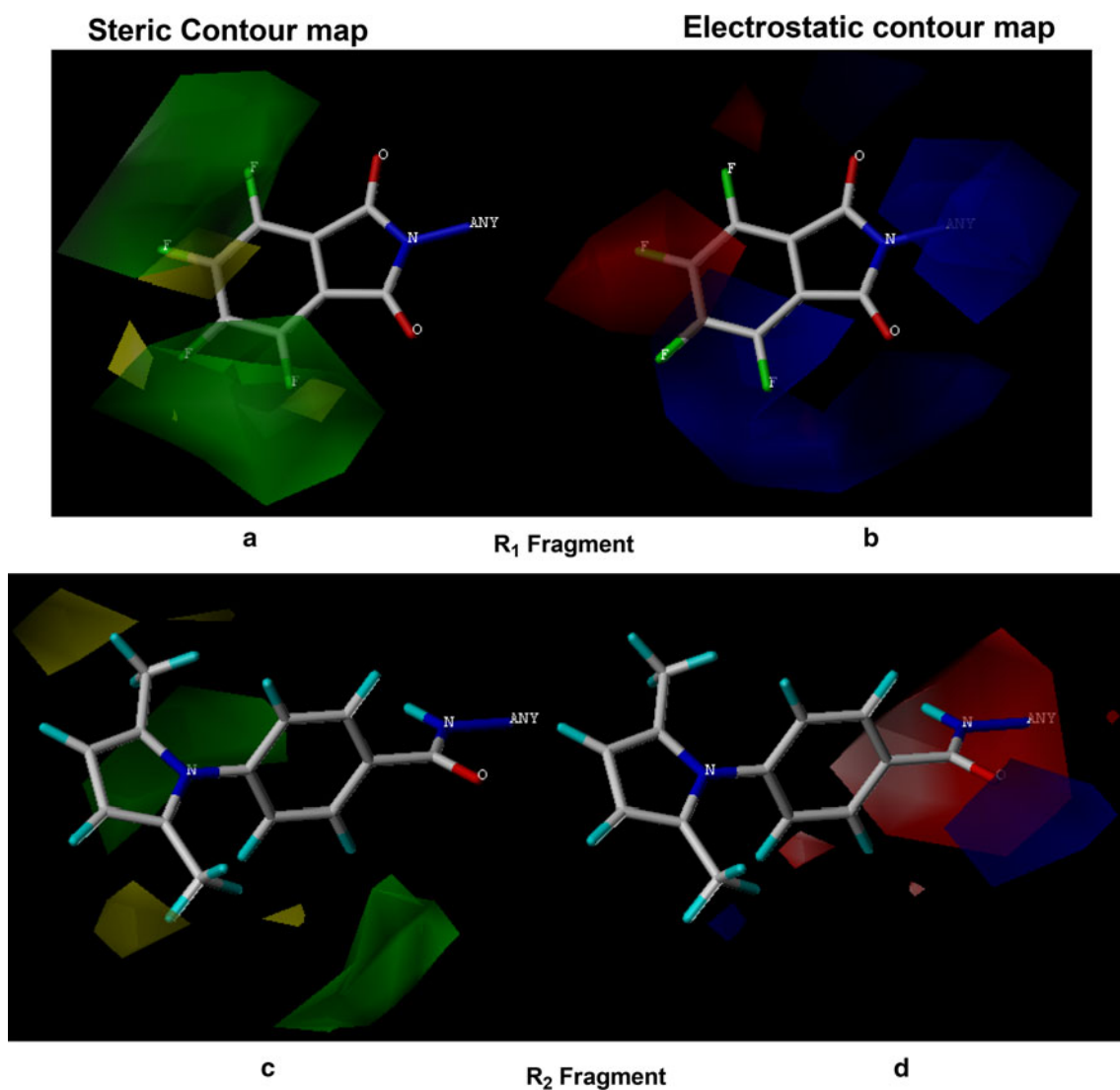


Fig. 7 Steric and electrostatics stdev* coefficient contour map for compound **8h** by Topomer CoMFA analysis. **a** Steric contour map for the R₁ fragment. **b** Electrostatic contour map for the R₁ fragment. **c** Steric contour map for the R₂ fragment. **d** Electrostatics contour map

for the R₂ fragment. Sterically favored/unfavored areas are shown in *green/yellow contour*, while the *blue/red polyhedra* depict the favorable sites for the positively/negatively charged groups (Color figure online)

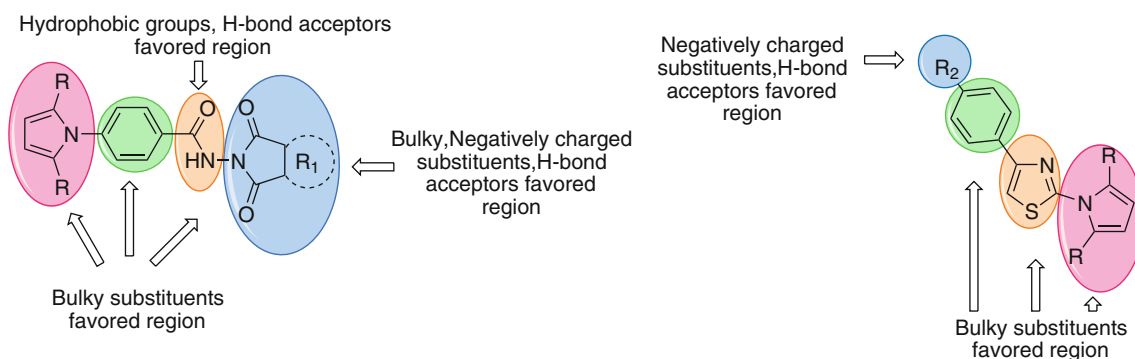


Fig. 8 Summary of structure–activity relationship

PLS results is provided in Table 5. The predictive ability of the developed Topomer CoMFA model was assessed by the test set (eight molecules) predictions, which were excluded during the Topomer CoMFA model generation. The predictive ability of the test set was 0.689. The actual and predicted activities of the training set and test set molecules along with R₁ and R₂ fragment contributions are given in Table 6. The graph of predicted versus actual activity for training set and test set molecules is shown in Fig. 3.

Contour map analysis Contour level along with color scheme and estimated volume of contour are summarized in Table 7. The 3D-QSAR contours and their relationship with the biological activity of molecule are described in Figs. 4, 5, 6, and 7. In the steric contour map, green color denotes sterically bulky groups favored for activity and the yellow color indicates sterically bulky groups unfavored for activity. In the electrostatics contour map, red indicates electronegative favored groups and blue indicates electropositive favored group. The steric contours of compound **13h** R₁ fragment (Fig. 4a) revealed that large green-colored contours favor the substitution of electronegative 4-fluoro group on phenyl moiety. The electrostatics contour map depicted that electronegative groups (red contour, Fig. 4b) are favored at the *para* position of phenyl group and hence, compound **13h** displayed the highest activity (pMIC = 6.70) among all the tested compounds in the series. For compounds **13b**, **d**, and **i** (pMIC = 6.40), the 4-fluoro group of compound **13h** was replaced by 4-chloro, 4-bromo, and 2,4-dichloro groups, respectively, that produced smaller inhibitory effect. Electropositive nature of the hydroxyl, methoxy, and amino groups was not favorable for activity when located at the 4-position on phenyl ring, but showed decreased inhibitory potency. For compound **13a**, the unsubstituted phenyl ring was less favored for activity and the compound displayed less inhibitory potency than **13h**. For the R₂ fragment, green contours (Fig. 4c) near the methyl group of pyrrole indicated that bulky group was favored for the inhibitory effect, while the red color near the thiazole indicated that an electronegative substitution could retain molecular activity.

Steric and electrostatic contour maps for compound **5h** are shown in Fig. 5. Fragment R₁ consisted of cyclic imide moiety. In the steric contour map (Fig. 5a), the green color indicates less bulky and electronegative group at the *ortho*, *meta*, and *para* positions at the phenyl group of cyclic imide moiety was favored for activity. The electrostatic contour map (Fig. 5b) revealed that electron withdrawing nature of fluorine group substituted at 4,5,6,7-positions of cyclic imide was favored for activity. The replacement of 4,5,6,7-tetrafluoro group of compound **5h** with 4,5,6,7-tetrabromo or tetrachloro group produced lesser inhibitory

effect. For compound **5e**, the unsubstituted phenyl ring was less favored for activity and the compound displayed less inhibitory potency than compound **5h**. For compounds **5j–l**, removal of halo groups from R₁ fragment produced a decreased activity compared to compound **5h**, indicating the necessity of the halo groups for the inhibitory effect. Compound **5i** showed better activity than compounds **5j–l** due to the presence of 5,6-dichloro group. In compound **5m**, the phenyl group of compound **5e** was replaced by the cyclohexyl group, which showed lesser inhibitory effect.

Steric and electrostatic contour maps for compound **12h** are shown in Fig. 6. Fragment R₂ consisted of hydrogen at the second and fifth positions of pyrrole ring. The steric contour map (Fig. 6c) revealed that the whole of pyrrole ring was favored for inhibitory potency. Fragment R₂ contribution in compounds **13a–l** revealed that bulky nature of 2,5-dimethylpyrrole ring was favorable for inhibitory potency than compounds **12a–l**.

Steric and electrostatic contour maps for compound **8h** are presented in Fig. 7. The steric contour map for fragment R₂ (Fig. 7c) revealed that phenyl group with pyrrole ring were favorable for activity. Fragment R₂ contribution in compounds **5a–m** revealed that 2,5-unsubstituted pyrrole ring was favorable for the inhibitory potency than the compounds **8a–m**.

Summary of structure–activity relationship The structure–activity relationship revealed by 3D-QSAR studies are illustrated in Fig. 8. According to Topomer CoMFA analysis, we observed that not only the negatively charged substituents, H-bond acceptors at R₁ and R₂ positions showed increase in activity (like in compounds **5h** and **13h**) but also the hydrophobic substituent at the position of the linker showed increased activity in cyclic imide series. The hydrophobic property of benzene, pyrrole, cyclic imide, and thiazole rings plays a key role in exhibiting antimycobacterial activities.

Conclusion

The present study reports on the synthesis of novel pyrrole derivatives and their in vitro antibacterial and antitubercular activities against MTB H₃₇Rv strain by broth dilution assay method have been evaluated. Among all the compounds, **5a**, **c**, **e**, **h**, **8h**, **12f**, **h**, **13f**, and **h** have shown better activity against the tested microorganisms and mycobacteria. Further, some of the compounds were assessed for their cytotoxicity (IC₅₀) against mammalian Vero cell lines and A₅₄₉ (lung adenocarcinoma) cell lines using the MTT assay method. The compounds exhibited antitubercular activity at non-cytotoxic concentrations. Some of the compounds of this study could be further developed as a

novel class of antibacterial and antitubercular agents, even though further structural modification is necessary. It was found that the 3D structural information is useful in drug design and the Topomer CoMFA model exhibited good internal and external consistency. The Topomer CoMFA model showed a good correlation between the actual and predicted values for training set molecules. The ability of QSAR model to accurately predict the property value (pMIC) along with other important information gathered from 3D contour maps are valuable in the design of new pyrrolylimides and pyrrolylthiazoles having improved antitubercular activity.

Acknowledgments Authors immensely thank the Indian Council of Medical Research, New Delhi, India for financial support [File No. 64/4/2011-BMS, IRIS Cell No. 2010-08710]. We also thank Dr. V. H. Kulkarni, Principal and Mr. H. V. Dambal, President, S.E.T.'s College of Pharmacy, Dharwad, India, for providing facilities. We thank Dr. K. G. Bhat, Maratha Mandal's Dental College, Hospital and Research Centre, Belgaum, India for providing facilities for antibacterial, antitubercular, and cytotoxic activities; Director, SAIF, Indian Institute of Technology, Chennai, Tamil Nadu, India and the Director, SAIF, Panjab University, Chandigarh, Panjab, India for providing the NMR and mass spectral data. We thank Mr. Shrikant A. Tiwari for his technical assistance.

References

- Abdel-Aziz AA (2007) Novel and versatile methodology for synthesis of cyclic imides and evaluation of their cytotoxic, DNA binding, apoptotic inducing activities and molecular modeling study. *Eur J Med Chem* 42:614–626
- Ahmadi A, Solati J, Hajikhani R, Pakzad S (2011) Synthesis and analgesic effects of new pyrrole derivatives of phencyclidine in mice. *Arzneimittelforschung* 61:296–300
- Biava M, Porretta GC, Poce G, Battilocchio C, Alfonso S, De Logu A, Serra N, Manetti F, Botta M (2010) Identification of a novel pyrrole derivative endowed with antimycobacterial activity and protection index comparable to that of the current antitubercular drugs streptomycin and rifampin. *Bioorg Med Chem* 18:8076–8084
- Borchhardt DM, Andricopulo AD (2009) CoMFA and CoMSIA 3D QSAR models for a series of cyclic imides with analgesic activity. *Med Chem* 5:66–73
- Bush BL, Nachbar RB Jr (1993) Sample-distance partial least squares: PLS optimized for many variables, with application to CoMFA. *J Comput-Aided Mol Des* 7:587–619
- Cramer RD (1993) Partial Least Squares (PLS): its strengths and limitations. *Perspect Drug Discov Des* 1(2):269–278
- Cramer RD (2003) Topomer CoMFA: a design methodology for rapid lead optimization. *J Med Chem* 46(3):374–388
- Cramer RD, Patterson DE, Bunce JD (1988) Comparative molecular field analysis (CoMFA). 1. Effect of shape on binding of steroids to carrier proteins. *J Am Chem Soc* 110:5959–5967
- Cramer RD, Clark RD, Patterson DE, Ferguson AM (1996) Bioisosterism as a molecular diversity descriptor: steric fields of single “topomeric” conformers. *J Med Chem* 39(16):3060–3069
- Dickey JB, Towne EB, Bloom MS, Moore WH, Hill HM, Heynemann H, Hedberg DG, Sievers DC, Otis MV (1959) Azo dyes from substituted 2-aminothiazoles. *J Org Chem* 24(2):187–196
- Duncan K, Barry CE (2004) Prospects for new antitubercular drugs. *Curr Opin Microbiol* 7:460–465
- Franzblau SG, Witzig RS, McLaughlin JC, Torres P, Madico G, Hernandez A, Degnan MT, Cook MB, Quenzer VK, Ferguson RM, Gilman RH (1998) Rapid, low-technology MIC determination with clinical *Mycobacterium tuberculosis* isolates by using the microplate Alamar Blue assay. *J Clin Microbiol* 36:362–366
- Gorczynski MJ, Leal RM, Mooberry SL, Bushweller JH, Brown ML (2004) Synthesis and evaluation of substituted 4-aryloxy- and 4-arylsulfanyl-phenyl-2-aminothiazoles as inhibitors of human breast cancer cell proliferation. *Bioorg Med Chem* 12:1029–1036
- Goto S, Jo K, Kawakita T, Mitsuhashi S, Nishino T, Ohsawa N, Tanami H (1981) Determination method of minimum inhibitory concentrations. *Chemotherapy* 29:76–79
- Gundersen LL, Nissen-Meyer J, Spilsberg B (2002) Synthesis and antimycobacterial activity of 6-arylpyrimidines: the requirements for the N-9 substituent in active antimycobacterial pyrimidines. *J Med Chem* 45:1383–1386
- Jones RA (1992) Pyrroles, Vinyl Pyrroles, Part II, the chemistry of heterocyclic compounds, vol 48. Wiley, New York, pp 131–298
- Jones RA, Bean GP (1997) The chemistry of pyrroles. Academic Press, London, pp 51–57
- Joshi SD, Vagdevi HM, Vaidya VP, Gadaginamath GS (2008) Synthesis of new 4-pyrrol-1-yl benzoic acid hydrazide analogs and some derived oxadiazole, triazole and pyrrole ring systems, a novel class of potential antibacterial and antitubercular agents. *Eur J Med Chem* 43:1989–1996
- Joshi SD, Joshi A, Vagdevi HM, Vaidya VP, Gadaginamath GS (2010) Microwave assisted synthesis of some new quinolinyl-pyrrole derivatives as potential antibacterial and antitubercular agents. *Indian J Heterocycl Chem* 19:221–224
- Joshi SD, More Y, Vagdevi HM, Vaidya VP, Gadaginamath GS, Kulkarni VH (2013a) Synthesis of new 4-(2,5-dimethylpyrrol-1-yl)4-pyrrol-1-yl benzoic acid hydrazide analogs and some derived oxadiazole, triazole and pyrrole ring systems a novel class of potential antibacterial, antifungal and antitubercular agents. *Med Chem Res* 22:1073–1089
- Joshi SD, Manish K, Badiger A (2013b) Synthesis and evaluation of antibacterial and antitubercular activities of some novel imidazo[2,1-b][1,3,4]thiadiazole derivatives. *Med Chem Res* 22:869–878
- Kamal A, Ramakrishna G, Lakshma Nayak V, Raju P, Subba Rao AV, Viswanath A, Vishnuvardhan MV, Ramakrishna S, Srinivas G (2012) Design and synthesis of benzo[c,d]indolone-pyrrolo-benzodiazepine conjugates as potential anticancer agents. *Bioorg Med Chem* 20:789–800
- Mohamed MS, Kamel R, Fathallah SS (2011) Synthesis of new pyrroles of potential anti-inflammatory activity. *Arch Pharm (Weinheim)* 12:830–839
- Mosmann T (1983) Rapid colorimetric assay for cellular growth and survival: application to proliferation and cytotoxicity assays. *J Immunol Methods* 65:55–63
- Pattan SR, Ali MS, Pattan JS, Purohit SS, Reddy VVK, Nataraj BR (2006) Synthesis and microbiological evaluation of 2-acetanilido-4-arylthiazole derivatives. *Indian J Chem* 45(B):1929–1932
- Sbardella G, Mai A, Artico M, Loddo R, Setzuc MG, La Colla P (2004) Synthesis and in vitro antimycobacterial activity of novel 3-(1*H*-pyrrol-1-yl)-2-oxazolidinone analogues of PNU-100480. *Bioorg Med Chem Lett* 14:1537–1541
- Singh D, Srivastava M, Gyananchandran AK, Gokulan PD (2010) Synthesis and biological evaluation of some new phenylthiazole derivatives for their antimicrobial activities. *J Curr Pharm Res* 4:16–19

- Tripes International (2012) Sybyl-X 2.0. Tripes International, St. Louis
- Valadas E, Antunes F (2005) Tuberculosis, a re-emergent disease. *Eur J Radiol* 55:154–157
- Vicini P, Geronikaki A, Incerti M, Busonera B, Poni G, Cabras CA, La Colla P (2003) Synthesis and biological evaluation of benzo[d]isothiazole, benzothiazole and thiazole Schiff bases. *Bioorg Med Chem* 11:4785–4789
- World Health Organization (2008) Global tuberculosis control: surveillance, planning, and financing, WHO Report. WHO Press, Geneva